



8-1983

A Microprocessor Controlled Pulsed Hollow Cathode Lamp for an Atomic Absorption Spectrometer

James B. Schilling

Follow this and additional works at: https://scholarworks.wmich.edu/masters_theses

 Part of the Analytical Chemistry Commons

Recommended Citation

Schilling, James B., "A Microprocessor Controlled Pulsed Hollow Cathode Lamp for an Atomic Absorption Spectrometer" (1983). *Master's Theses*. 1660.

https://scholarworks.wmich.edu/masters_theses/1660

This Masters Thesis-Open Access is brought to you for free and open access by the Graduate College at ScholarWorks at WMU. It has been accepted for inclusion in Master's Theses by an authorized administrator of ScholarWorks at WMU. For more information, please contact wmu-scholarworks@wmich.edu.



A MICROPROCESSOR CONTROLLED PULSED HOLLOW
CATHODE LAMP FOR AN ATOMIC ABSORPTION SPECTROMETER

by

James B. Schilling

A Thesis
Submitted to the
Faculty of The Graduate College
in partial fulfillment of the
requirements for the
Degree of Master of Arts
Department of Chemistry

Western Michigan University
Kalamazoo, Michigan
August 1983

A MICROPROCESSOR CONTROLLED PULSED HOLLOW CATHODE LAMP FOR AN ATOMIC ABSORPTION SPECTROMETER

James B. Schilling, M.A.

Western Michigan University, 1983

A Jarrell-Ash Atomic Absorption/Flame Emission 82-360 Spectrometer was interfaced to a Heathkit ETA-3400 microprocessor. The microprocessor is used to pulse the hollow cathode lamp from a "steady" current to a "peak " current during the opening of the chopper. The current from the photomultiplier tube is converted to a proportional voltage which is supplied to a sample-and-hold circuit. A successive approximation routine is used to convert the voltage to a representative digital value. Digital values are obtained for the "blank" and "sample" and are used to calculate percent absorption values. The system can also be used to obtain emission values.

The system was used to determine the concentration of chromium and nickel in steel by the "standard addition method". A slight loss in sensitivity was found at higher lamp intensities.

ACKNOWLEDGEMENTS

I would like to thank Dr. James Howell for his guidance and patience throughout the course of this research. His expertise in A.A.S. and microprocessors was very beneficial during the times of confusion. Also, I would like to extend my appreciation to Dr. Robert Anderson, Dr. Adli Kana'an, Dr. Robert Nagler, and Dr. Ralph Steinhaus for the guidance they gave me during the period of time I was at Western. I also deeply appreciate the support given to me by the Chemistry Department in the form of assistantships and funds for supplies.

Not enough thanks can be given to my parents and friends whose moral support was crucial to obtaining this degree

James B. Schilling

INFORMATION TO USERS

This reproduction was made from a copy of a document sent to us for microfilming. While the most advanced technology has been used to photograph and reproduce this document, the quality of the reproduction is heavily dependent upon the quality of the material submitted.

The following explanation of techniques is provided to help clarify markings or notations which may appear on this reproduction.

1. The sign or "target" for pages apparently lacking from the document photographed is "Missing Page(s)". If it was possible to obtain the missing page(s) or section, they are spliced into the film along with adjacent pages. This may have necessitated cutting through an image and duplicating adjacent pages to assure complete continuity.
2. When an image on the film is obliterated with a round black mark, it is an indication of either blurred copy because of movement during exposure, duplicate copy, or copyrighted materials that should not have been filmed. For blurred pages, a good image of the page can be found in the adjacent frame. If copyrighted materials were deleted, a target note will appear listing the pages in the adjacent frame.
3. When a map, drawing or chart, etc., is part of the material being photographed, a definite method of "sectioning" the material has been followed. It is customary to begin filming at the upper left hand corner of a large sheet and to continue from left to right in equal sections with small overlaps. If necessary, sectioning is continued again—beginning below the first row and continuing on until complete.
4. For illustrations that cannot be satisfactorily reproduced by xerographic means, photographic prints can be purchased at additional cost and inserted into your xerographic copy. These prints are available upon request from the Dissertations Customer Services Department.
5. Some pages in any document may have indistinct print. In all cases the best available copy has been filmed.

**University
Microfilms
International**

300 N. Zeeb Road
Ann Arbor, MI 48106

▼

✓

✓

1321907

SCHILLING, JAMES BOYD

A MICROPROCESSOR CONTROLLED PULSED HOLLOW CATHODE LAMP
FOR AN ATOMIC ABSORPTION SPECTROMETER

WESTERN MICHIGAN UNIVERSITY

M.A.

1983

University
Microfilms
International 300 N. Zeeb Road, Ann Arbor, MI 48106

—

TABLE OF CONTENTS

ACKNOWLEDGEMENTS	ii
LIST OF TABLES	v
LIST OF FIGURES	vi
Chapter	
I. INTRODUCTION	1
History of Atomic Absorption Spectroscopy	1
Theory	3
II. SOURCES	5
Types of Sources	5
Pulsed Hollow Cathode Lamps	7
III. THE JARRELL-ASH ATOMIC ABSORPTION/FLAME EMISSION SPECTROMETER	10
IV. MICROPORCESSOR CONTROLLED PULSED HOLLOW CATHODE LAMP. .	11
Theoretical Considerations	13
Heathkit ETA-3400 Trainer with Memory I/O Accessory . .	16
MC6821P Peripheral Interface Adapter	16
Digital to Analog Conversion	19
Pulsed Hollow Cathode Lamp Power Supply	20
Detector for Phasing of Chopper	22
Amplification of the Signal from the PMT	23
Analog to Digital Conversion	24
V. SOFTWARE DEVELOPMENT - 6800 MACHINE LANGUAGE	28
The Main Machine Language Routine	28

Initialization Subroutine	30
Wait for the Chopper to Open Subroutine	30
Wait for the Chopper to Close Subroutine	31
Data Acquisition Subroutine	31
Store Data Point Subroutine	32
Addition Subroutine	33
Division Subroutine	33
VI. SOFTWARE DEVELOPMENT - HEATHKIT TINY BASIC	35
Tiny Basic Main Routine	35
%A and Emission Calculation	36
Data Acquisition Subroutine	37
VII. RESULTS AND CONCLUSIONS	38
Determination of Chromium and Nickel in Steel	45
APPENDICES	
Appendix A. Machine Language Routine Flowcharts	48
Appendix B. Tiny Basic Routine Flowcharts	55
Appendix C. Machine Language Program	59
Appendix D. Tiny Basic Program	67
Appendix E. Memory Chart	70
Appendix F. Timing Diagram	72
Appendix G. PMT Dynode Voltage vs. Measured Lamp Intensity for Co, Cu, and Ni	74
REFERENCES	79

LIST OF TABLES

1.	Bit Assignment of Port \$4000 of PIA 2	29
2.	Effect of Increased Emission from the Pulsed Hollow Cathode Lamp on Cobalt, Nickel, and Copper Calibration Curves	39
3.	Regression Analysis of Emission Calibration Curves for Copper and Calcium	41
4.	Regression Analysis of Calibration Curves for Copper and Cobalt Using Pulsed A.A.	42
5.	Regression Analysis of Calibration Curves for Chromium Regular and Pulsed A.A.	43
6.	Regression Analysis of Calibration Curves for Nickel Regular and Pulsed A.A.	43
7.	Regression Analysis of Calibration Curves for Silver Regular and Pulsed A.A.	44
8.	Results and Regression Analysis of Standard Addition Curves for Chromium in Steel by Pulsed A.A.	46
9.	Results and Regression Analysis of Standard Addition Curves for Nickel in Steel by Pulsed A.A.	47

LIST OF FIGURES

1.	Block diagram of the microprocessor controlled pulsed . . .	12
	hollow cathode lamp instrument	
2.	Schematic diagram for connection of PIA 1 to the	
	Heathkit ETA-3400 MPU	17
3.	Schematic diagram for the hollow cathode lamp power	
	supply	21
4.	Schematic diagram of the IR trnasistor detector	
	for phasing of chopper	23
5.	Amplifier circuit for the current signal from the	
	photomultiplier tube	24
6.	Sample and hold curcuit	26
G1.	Plot of the dynode voltage of the PMT vs. the	
	measured intensity of the Nickel hollow cathode lamp . . .	75
G2.	Plot of the dynode voltage of the PMT vs. the	
	measured intensity of the Chromium hollow cathode lamp . .	76
G3.	Plot of the dynode voltage of the PMT vs. the	
	measured intensity of the Cobalt hollow cathode lamp . . .	77
G4.	Plot of the dynode voltage of the PMT vs. the	
	measured intensity of the Copper hollow cathode lamp . . .	78

CHAPTER I

INTRODUCTION

The light source commonly used in Atomic Absorption Spectroscopy is the hollow cathode lamp. In order to maximize the lifetime of this lamp, it should be operated with a continuous current that is less than or equal to the manufacturer's suggested maximum value. As a result, it has limited intensity and a lower than desired signal to noise ratio (S/N). The purpose of this paper is to describe a microprocessor controlled system in which the intensity of the common hollow cathode lamp is increased by pulsing it with high currents. Short duration pulses of the lamp provides a time averaged current which is less than the maximum continuous current specified by the manufacturer.

History of Atomic Absorption Spectroscopy

The history of Atomic Absorption Spectroscopy (AAS) is well documented in the literature (1,2,3). Sir Issac Newton(1) in 1672, described the use of a prism to disperse sunlight into its spectrum. The first evidence of the occurrence of atomic absorption, though it was not understood as such, was provided by Wollaston(1) in 1802 with his description of the dark lines in the solar spectrum. The wavelengths of these lines were later measured by Fraunhofer(1) in 1817. It was not until 1860 that the concept of atomic absorption was completely

elucidated by Bunsen and Kirchoff(1,2). From 1860 to 1953 AAS was primarily used by astronomers for the identification of elements in the stars, and by laboratory personnel for the detection of mercury vapors. Atomic emission spectroscopy was by far favored over AAS as the method for the quantitative analysis of trace elements during this period.

In 1953 Walsh (4) described the general utility of atomic absorption spectrometer analyses in the laboratory. Later, (5) he patented a laboratory instrument for making these measurements. With this event the use of AAS increased rapidly. However, to date, improvements in the technique have been in only four areas. The first of these is the use of a nitrous-oxide/acetylene flame for the detection of refractory elements. The second is the increased sensitivity to trace elements by as much as 1000 fold through the use of electrothermal analyzers. These analyzers often encounter numerous and complex interferences. Consequently, the flame still retains much of its popularity as a simple low cost atomic vapor generator. The third area of improvement is the increased ability to control operating parameters and handle large quantities of data through the use of microcomputers. The Perkin-Elmer Model 5000 Atomic Absorption Spectrometer, for example, with its automated sample handling capabilities can determine six elements in fifty samples in less than thirty five minutes. The fourth area of improvement has been the use of a reference beam to compensate for interferences due to deviations in the power supply of the hollow cathode lamp and due to scattering and absorption by matrix species in the flame. The Zeeman effect and

continuous source correction techniques are two examples of this concept.

Theory

An essential requirement for analytically useful absorption and emission of an analyte is the production of free atoms in the flame. To achieve this, a solution may be nebulized to a uniformly sized aerosol of about two micrometers in diameter which are efficiently mixed with oxidant and fuel. The flame temperature must be sufficiently high to completely desolvate, decompose, and vaporize the droplets to produce atomic vapor. Once in this state, the atoms are capable of absorption and emission at resonance frequencies. The number of atoms in an excited state due to absorption or thermal excitation is small compared to that remaining in the ground state at any given instance. The ratio of excited state atoms to ground state atoms for a given temperature can be calculated from the Boltzmann distribution equation.

Emission intensity is proportional to the number of atoms in the excited state and is, therefore, highly dependent upon the temperature of the flame. Calibration curves are used to relate concentration to emission intensity. These curves are normally nonlinear due to spectral and chemical interferences.

The degree of absorption is dependent upon the number of atoms in the ground state and upon the oscillator strength of the atoms. The Beer-Lambert law is used to relate absorbance to concentration. Deviations from this law occur since there is never really a steady

state of homogeneously distributed atoms in the flame. Also the effect of spectral and chemical interferences which are commonly present tend to give rise to deviations from the law. As a result, calibration curves are frequently used. When complex matrices are studied difficulties in obtaining a well matched blank may make it advantageous to use either the "standard addition method" or the "internal standard method".

CHAPTER II

SOURCES

The source used in AAS must provide a stable and intense emission line of narrow band width. It must also minimize effects which may cause decreased sensitivities, such as, Doppler and Lorentz broadenings, self absorption, and line reversal.

Types of Sources

The hollow cathode lamp meets most of the requirements of a good source. However, limitations are evident with those lamps having cathodes made up of elements having high vapor pressures since they are more susceptible to self absorption. The intensity of the hollow cathode lamp is governed by the low operating currents required. If the current is increased, self absorption and line broadening become prominent due to the accompanying increase in the vapor pressure and density of the atom cloud within the lamp. Pulsed lamps have been successful in increasing the intensity by 50 to 200 fold. These methods will be discussed in greater detail later.

High intensity sources are desired because they achieve high S/N ratios and, therefore, improved detection limits. The high intensity hollow cathode lamp was developed for this purpose. Its design is similar to the common hollow cathode lamp except that it has two extra electrodes which produce a high density electron region that

serves to excite the atom cloud. These lamps have less line reversal and produce more stable signals than the common hollow cathode lamps. Spectral lines from ions are more suppressed with these lamps also.

Because of the expense of having to have a separate lamp for each element, the demountable hollow cathode lamp was developed. This lamp has replaceable cathodes for each element. Its performance is comparable to the common hollow cathode lamp. However, it has the disadvantage of being inconvenient due to the need for it to be evacuated and refilled with an inert gas to a low precise pressure each time the electrodes are changed.

Gaseous discharge lamps were developed for elements such as cadmium and mercury that have high vapor pressures. These lamps produce very intense resonance lines and few, if any, ion lines. The resonance lines are affected by reversal and broadening. However, these effects can be reduced, to some extent, by lowering the supply voltage to the lamp.

Electrodeless discharge lamps produce narrow lines of high intensities with very little self absorption. The performance of these lamps depends upon the pressure of the fill gas, the lamp dimensions, and the operating temperature. The stability of these lamps is not as good as that of the common hollow cathode lamp although they generally have lower detection limit capabilities as a result of their high intensities (6,7).

Pulsed Hollow Cathode Lamps

In 1967 Dawson and Ellis (8) reported obtaining a 50 to 500 fold increase in the resonance line emission from a conventional hollow cathode lamp by pulsing it with high currents (300 to 600 milliamps) for short periods of time (15 to 40 microseconds). The resonance lines produced showed little self absorption and only minimal changes in line width and reversal. Pulse current, which is the maximum, or peak, current supplied to the lamp, and steady current, which is supplied to the lamp intermittent to the pulses, were found to be the two most important optimizing parameters. Upon increasing the pulse current it was found that the light output was enhanced and the detection limits improved. There was, however, some loss of sensitivity. Upon increasing the steady current there was found to be a loss of light output and only slight changes in sensitivity and detection limits. Other parameters such as pulse width and pulsing frequency were found to have little effect on the sensitivity and detection limits. The major advantages of the use of pulsed hollow cathode lamps as seen by Dawson and Ellis were:

1. S/N was increased by 50 to 500 fold.
2. The use of narrower slit widths was possible due to the increased intensity of the emission resonance line
3. The operation of the lamp was less critically dependent upon the filler gas pressure which resulted in a longer lamp life and a more rapid warm up time.

Since the work of Dawson and Ellis several applications for pulsed hollow cathode lamps have been developed. Kitagawa and associates (9) combined these lamps with instrumentation for atomic

magneto-optical rotation spectroscopy for the trace analysis of elements such as Sb, Bi, Ag, and Cu. They also discovered that not only did the time averaged current affect the lamp life but also the peak current. They discovered that physical damage to the cathode of a Ag lamp developed in about one half the length of time guaranteed for the normal continuous operation when a peak current of 200 milliamps and a time averaged current of 10 milliamps were used.

DeJong and Piepmeir (10,11) used copper and silver pulsed hollow cathode lamps in combination with a piezoelectrically driven interferometer to obtain time- and wavelength- resolved emission line profiles of these elements. Through this work they discovered that line reversal was enhanced earlier in the time period of a pulse as higher peak currents were used. Using a lamp driven at 100 Hertz with pulses of 300 microseconds in duration and 400 milliamp peaks, they discovered that extreme reversal occurred after the first 100 microseconds in the copper lamp. The silver lamp showed extreme reversal during the first 21 microseconds.

Osten and Piepmeir (12) demonstrated the applicability of the pulsed hollow cathode lamp for the measurement of atomic absorption in a laser plume. They discovered that the uncertainty due to shot noise was 7 to 14 times less when using a pulsed lamp as compared to that obtained with a nonpulsed.

Pulsed hollow cathode lamps have also been used in background correction techniques. Araki and associates (13) took advantage of the presence of ion lines in the spectrum produced by the hollow cathode lamp in the development of their dual wavelength background correction

method. They monitored the emission of both the resonance line and an adjacent ion line during the pulsed and nonpulsed periods. Ratios were taken of the pulsed and nonpulsed signals for each line which corrected for background interferences.

Pulsed hollow cathode lamps have been used in atomic fluorescence spectroscopy (14). Cardos and Malmstadt (15,16) described the use of an intermittent pulsing method in the operation of the hollow cathode lamp with high currents of about 200 milliamps. The use of a timing sequence produced short term stabilities of 0.08% and long term stabilities of 0.2%.

Johnson, Mann, and Vickers (17) have described a system which provides complete control of the important current waveform variables in the operation of pulsed hollow cathode lamps. A closed loop system based on a simplex optimization technique was utilized to determine the best values for the peak, time averaged, and steady currents as well as the intermittent times between pulses.

Jenke and Woodriff (18) utilized a background emission correction technique developed by Dewalt and associates (19) and a pulsed hollow cathode lamp to produce a system which simultaneously obtains measurements of analyte emission and absorption in a constant temperature furnace. The system gave excellent sensitivities, in the parts per billion range, for both emission and absorption of the analytes Cd, Mn, Mg, and Ni. The linear concentration ranges obtained were over five orders of magnitude for both emission and absorption of these analytes.

CHAPTER III

THE JARRELL-ASH ATOMIC ABSORPTION/FLAME EMISSION SPECTROMETER

A Jarrell-Ash Atomic Absorption/Flame Emission 82-360 spectrometer was used in this research. This instrument is composed of a 650 VDC current regulated hollow cathode lamp power supply, a lamp turret, a rotating disk chopper, a 0.5 meter Ebert scanning monochromator, and a sensitive AC amplifier for the detection of small currents from the photomultiplier. The 0.5 meter Ebert scanning monochromator utilizes a 1180 groove per millimeter grating which provides a linear dispersion of 16 angstroms per millimeter and a resolution of 0.2 angstroms in the first order. Modifications to the basic unit include periscope optics, a Keithly Model 244 high voltage power supply for the photomultiplier tube, and a 1P28 photomultiplier. The light from the hollow cathode lamp is modulated at 90 Hertz by the rotating disk chopper. A second chopper placed between the burner and the entrance slit to the monochromator can be used in emission analyses.

CHAPTER IV

MICROPROCESSOR CONTROLLED PULSED HOLLOW CATHODE LAMP

The block diagram of the instrument developed is given in Figure 1.

The Heathkit ETA-3400 MPU with memory accessory is interfaced to two Motorola MC6821P peripheral interface adapters (PIA). Ports A and B of PIA 1 have the assigned addresses \$8000 and \$8002, respectively. Ports A and B of PIA 2 have the assigned addresses \$4000 and \$4002, respectively. Throughout the rest of this text the address values given can be assumed to be hexadecimal (designated by \$) unless otherwise specified and the ports of the PIAs will be referred to by their addresses. The outputs of \$8002 and \$4002 are converted by digital to analog converters, D/A 1 and D/A 2, to representative negative voltages. The voltages are made positive by inverters I-1 and I-2, respectively, and then supplied to the input of the summing amplifier. The voltage supplied from D/A 1 (\$8002) can be connected or disconnected from the summing amplifier by means of the analog switch which is opened and closed by the pulse signal obtained from bit 3 of \$4000. When both D/A voltage outputs are supplied to the summing amplifier, the peak current is supplied to the hollow cathode lamp. When the analog switch is open only the steady current drives the lamp.

To detect when the chopper is opened or closed an infrared transistor detector system is utilized. The signal from this detector is

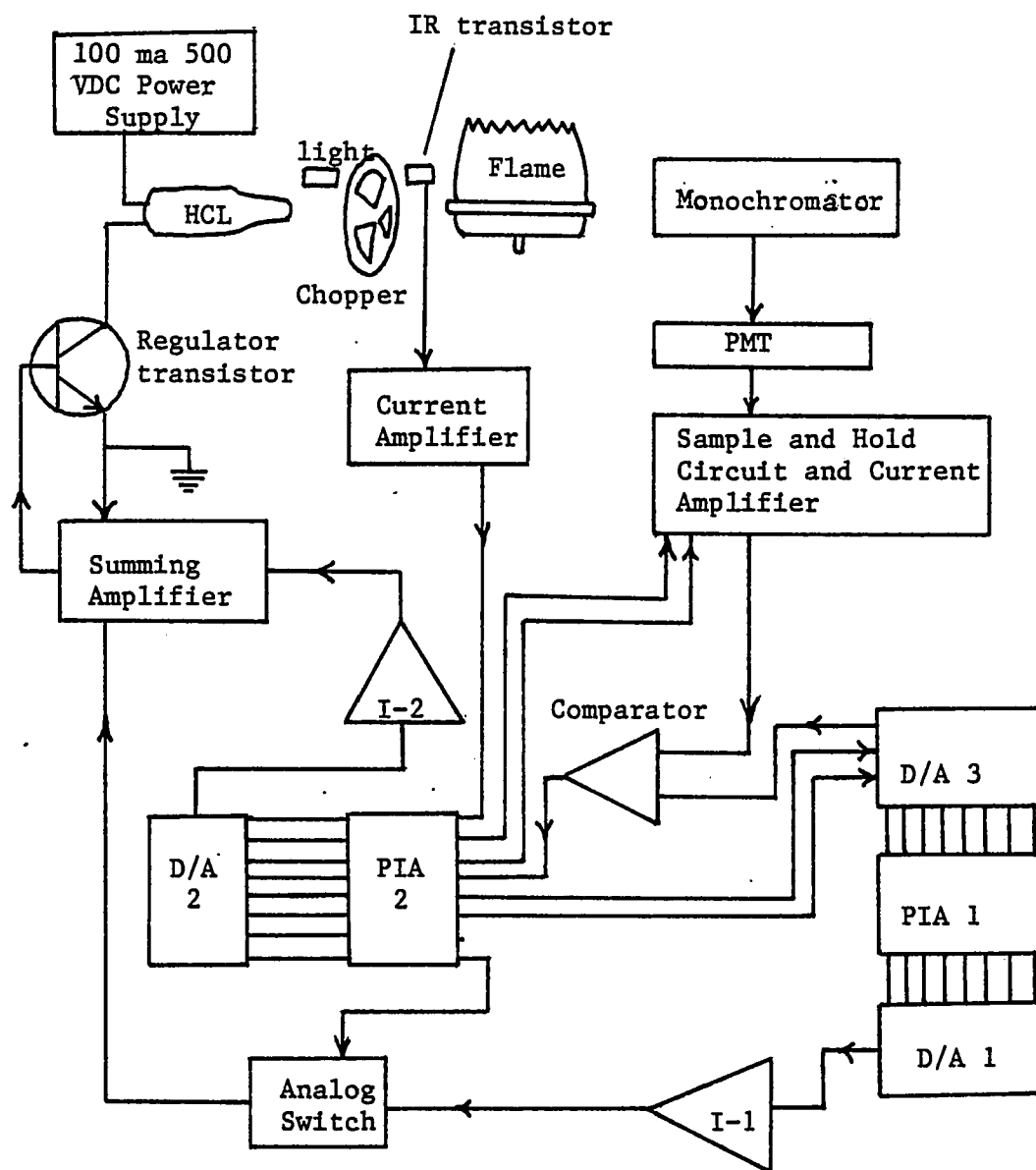


Figure 1. Block diagram of the microprocessor controlled pulsed hollow cathode lamp instrument.

either 5 volts or 0 volts and is supplied to bit 4 of \$4000.

The light from the hollow cathode lamp passes through a 0.5 meter Ebert monochromator and is detected by a 1P28 photomultiplier tube (PMT). The current from the PMT is amplified by a current-to-voltage converter to a proportional voltage which is supplied to the capacitor of a sample-and-hold circuit. The signal from bit 7 of \$4000 controls the time the capacitor is allowed to charge. After this period of time the capacitor voltage is compared to a reference voltage supplied by a 10-bit D/A converter (D/A 3). The D/A converter's output voltage is set by the digital values in \$8000 (8 bits) and \$4000 (2 bits). These digital values are varied by a successive approximation software routine. When the reference voltage becomes larger or smaller than the capacitor voltage the comparator's output state is changed causing the setting or clearing of bit 5 of \$4000. A ten bit binary data value representative of the capacitor voltage is obtained after completion of the routine. Before another value is obtained a signal from bit 6 of \$4000 causes the capacitor to discharge.

A Lear-Seigler ADM cathode ray tube (CRT) terminal is interfaced to the microprocessor by means of a RS232 interface provided in a Heath Model ETA-3400 memory I/O accessory. This provides the operator with a visual display of the data and program listings.

Theoretical Considerations

The following is the development of the equation for percent absorption (%A) in terms of the components that comprise the signal produced by the photomultiplier tube. At any given time the signal

produced by the PMT can be representative of one of ten possible conditions.

Condition 1. The entrance slit to the monochromator is covered so that no light may enter. The only signal produced by the PMT should, therefore, be only dark current.

$$S(0) = \text{Dark Current} \quad (1)$$

Condition 2. The chopper is closed and no sample or blank is aspirated into the flame. The resultant signal from the PMT is due to the combination of $S(0)$ and the current produced through the detection of the emission of the flame background $P(\text{FB})$.

$$S(1) = P(\text{FB}) + S(0) \quad (2)$$

Condition 3. No sample or blank is aspirated into the flame, the chopper is open, and the lamp is at its steady current $P(S)$.

$$S(2) = P(S) + P(\text{FB}) + S(0) \quad (3)$$

Condition 4. This is similar to Condition 3 except the lamp is at its peak current $P(S) + P(P)$.

$$S(3) = P(S) + P(P) + P(\text{FB}) + S(0) \quad (4)$$

Condition 5. Blank is aspirated into the flame and the chopper is closed.

$$S(4) = P(\text{FMB}) + S(0) \quad (5)$$

Where $P(\text{FMB})$ is the flame matrix background emission.

Condition 6. This is similar to Condition 5 except the chopper is open and the lamp is at its steady current.

$$S(5) = P(S) + P(\text{FMB}) + S(0) \quad (6)$$

Condition 7. Blank is aspirated into the flame, the chopper is open, and the lamp is at its peak current.

$$S(6) = P(S) + P(P) + P(\text{FMB}) + S(0) \quad (7)$$

Condition 8. Sample is aspirated into the flame and the chopper is closed. $P(E)$ is the emission due to the sample.

$$S(7) = P(\text{FMB}) + P(E) + S(0) \quad (8)$$

Condition 9. This is similar to Condition 8 except the chopper is open and the lamp is at its steady current.

$$S(8) = P(S^*) + P(FMB) + P(E) + S(0) \quad (9)$$

$$\text{Where } P(S^*) = P(S) - \text{fraction absorbed} \quad (10)$$

Condition 10. This is similar to Condition 9 except the lamp is at its peak current.

$$S(9) = P(P^*) + P(S^*) + P(FMB) + P(E) + S(0) \quad (11)$$

$$\text{Where } P(P^*) = P(P) - \text{fraction absorbed} \quad (12)$$

The defining equation for percent absorption (%A) is composed of two variables, P_o and P , which need to be determined from the previously defined equations.

$$\%A = (1 - (P/P_o)) \times 100 \quad (13)$$

P_o is the initial intensity of emission from the lamp and P is the intensity upon aspiration of the sample. The value of P_o is congruent to $P(S) + P(P)$ and can be obtained by subtracting $S(4)$ from $S(6)$.

$$P_o = P(S) + P(P) = S(6) - S(4) \quad (14)$$

The value of P is congruent to $P(P^*) + P(S^*)$ and can be obtained by subtracting $S(7)$ from $S(9)$.

$$P = P(P^*) + P(S^*) = S(9) - S(7) \quad (15)$$

As a result, four separate measurements must be made in the determination of the value of %A.

$$\%A = \left(1 - \frac{S(9) - S(7)}{S(6) - S(4)} \right) \times 100 \quad (16)$$

The values $S(9)$ and $S(7)$ are measured when the chopper is opened and closed, respectively, the sample is aspirated into the flame, and the lamp is at its peak current during the opening of the chopper. The values $S(6)$ and $S(4)$ are measured under exactly the same set of conditions except the blank is aspirated into the flame instead of the sample.

The emission value produced by aspirating the sample into the flame can be obtained by subtracting $S(4)$ from $S(7)$.

$$P(E) = S(7) - S(4) \quad (17)$$

Heathkit ETA-3400 Trainer with Memory I/O Accessory

The Heathkit ETA-3400 Trainer with ETA-3400 memory input/output accessory microprocessor system was utilized for data handling and peripheral device control.

The Motorola MC6808 central processing unit (CPU) permits the use of five addressing modes, two accumulators, an index register, and a stack pointer. All address, control and data busses are readily accessible through connections on the front panel of the trainer. The trainer, itself, provides only 512 bytes of random access memory (RAM). However, by addition of the memory accessory unit this can be expanded to 4096 bytes. The memory accessory unit also provides a Tiny Basic interpreter in read only memory (ROM), an RS232 interface for video terminal connection, and a cassette interface.

MC6821P Peripheral Interface Adapter

Two Motorola MC6821P peripheral interface adapters (PIA) are used to interface the external devices to the microprocessor. The pin assignments for the MC6821P are given in Figure 2.

Associated with each PIA are two eight bit input/output ports, A and B. Connections of data busses from external devices to these ports are made at pins PA0-PA7 and PB0-PB7, respectively. Data transfer between the PIA and the CPU is accomplished through a bidirectional

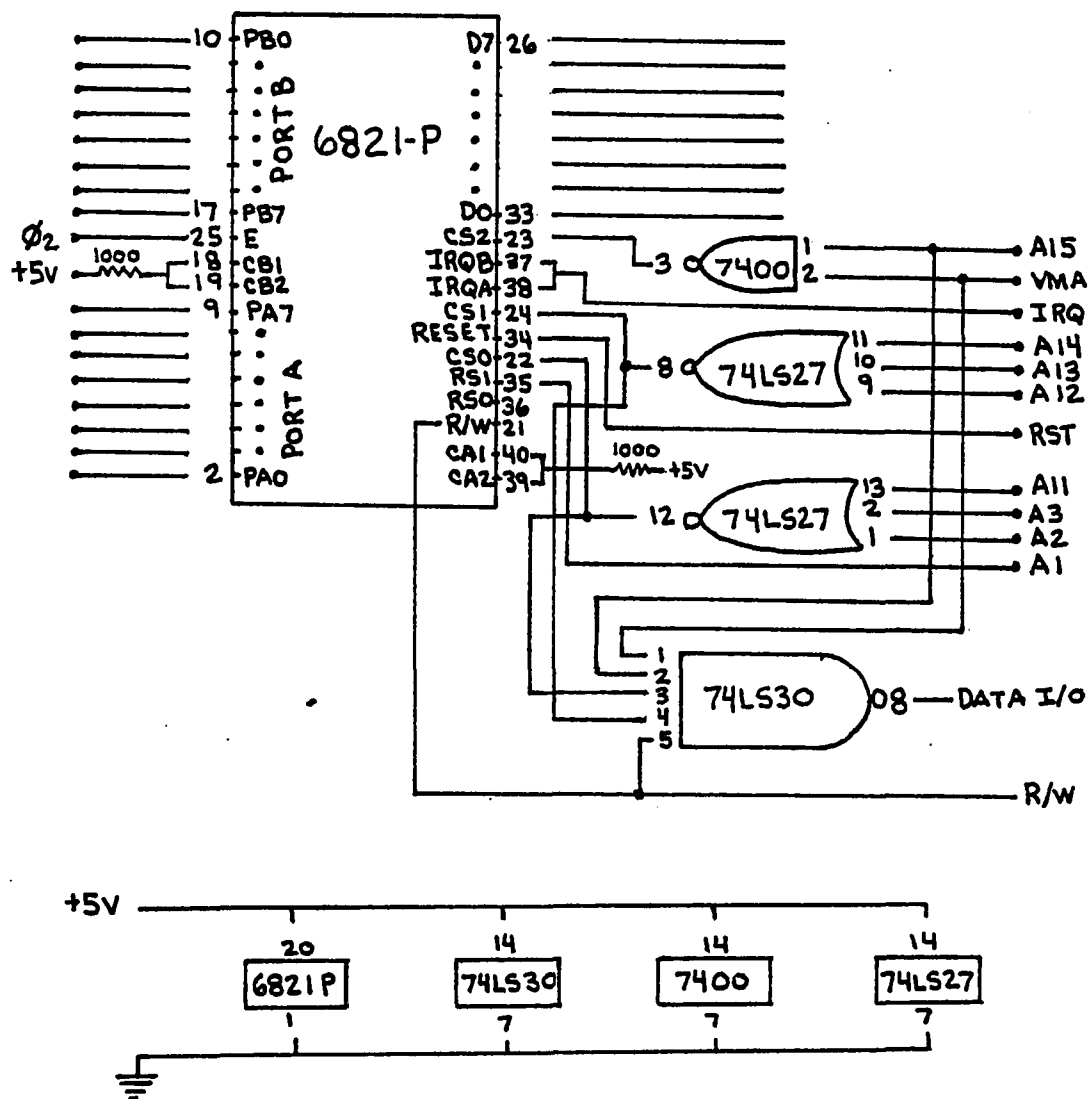


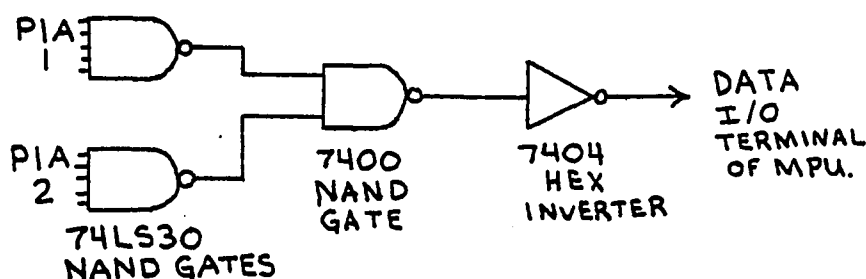
Figure 2. Schematic diagram for connection of PIA 1 to the Heathkit ETA-3400 MPU.

data bus that makes connections at pins D0-D7. Before any data transfer can take place the PIA must be selected through the appropriate signal levels on the address bus of the CPU, A0-A15. For the PIA to be selected, the device select signals CS0, CS1, and CS2 must be high, high, and low, respectively. The signals RS0 and RS1 address one of four memory locations associated with the PIA. CA1, CA2, CB1, and CB2 are timing and control signals required for interfacing the PIA to external logic. E and R/W are control signals associated with interfacing the PIA to the CPU. Each I/O port has associated with it an interrupt request signal, either IRQA or IRQB. The reset pin, Reset, with the appropriate level will clear all the PIA's registers.

The schematic diagram for the connection of one PIA to the microprocessor is given in Figure 2. Nine address lines and the VMA line supply the appropriate signals to logic circuitry to select the PIA. A15 and VMA are supplied to the inputs of a 7400 NAND gate. For CS2 to be the required low state, both A15 and VMA must be high. Address lines A12-A14 are supplied to the inputs of a three input NOR gate ($\frac{1}{2}$ - 74LS27). Only when all three of these inputs are low will CS1 be high. Address lines A1, A2, and A11 are supplied to the inputs of another three input NOR gate ($\frac{1}{2}$ - 74LS27). Likewise, for CS0 to be high all three inputs must be low. When CS2, CS1, and CS0 are at the described conditions the PIA is selected. When this occurs data transfer can take place between the PIA and the CPU. The direction of transfer is determined by the state of the R/W signal.

The modifications required for the connection of two PIAs to the microprocessor are as follows:

1. All interface connections to the microprocessor are connected in parallel (data bus lines, IRQ, RST, R/W and \emptyset_2).
2. All address lines are connected in parallel to the microprocessor. However, address lines A14 and A15 are interchanged in connection to PIA 2 for addressing purposes.
3. The following changes in the connection of the output of the 74LS30 NAND gate of each PIA are made:



Digital to Analog Conversion

The two major methods of D/A conversion are the weighted resistor ladder and the binary ladder network methods. The Heath Model EU-800-GC 10-bit D/A converter is based upon the latter of these. Three of these D/A converters are utilized in the instrument developed in this work. Two are used to generate the control voltages that determine the peak and steady currents that drive the hollow cathode lamp. The third D/A converter supplies the reference voltage that is used in the analog to digital conversion of the PMT current signal.

The EU-800-GC D/A converter can be used either in an output current mode or in an output voltage mode. The latter was used in all three cases. The output voltage range is 0 to -10 volts DC at 5 milliamps. The accuracy of conversion is ± 1 LSB (least significant bit), absolute and the linearity is within $\pm \frac{1}{2}$ LSB. The settling

time to 0.5% full scale is 25 microseconds for a 10 volt step. The zero offset is ± 1 LSB. The digital input can be either straight binary or signed complement. Negative logic determines the magnitude of the output. For example, a binary input of zero will cause the maximum voltage output of -10 volts. For the D/A converters that control the peak and steady currents only the eight least significant bits are used so that the maximum output is -2.49 volts. All ten bits are used by the D/A converter that provides the reference voltage for the A/D conversion.

Pulsed Hollow Cathode Lamp Power Supply

The pulsed hollow cathode lamp power supply schematic is shown in Figure 3. This supply is a modified version of that described by Dewalt, Amend, and Woodruff (20). Its major advantage over other supplies described (15,16, 21) lies in its long term stability, e.g., $\pm 0.0082\%$ over several hours. Unlike the circuit described by Dewalt and associates which utilized variable resistor pots to control the magnitude of the peak and steady currents, the circuit developed in this work utilizes two digital to analog converters whose outputs are controlled by the microprocessor. The voltage outputs of the two D/A converters are supplied to the inputs of unity gain inverters. The output of one inverter is connected to an analog switch which is opened and closed by a signal from the microprocessor. The peak current is supplied to the hollow cathode lamp when the switch is closed.

The first amplifier (OA-3) after the two inverters (OA-1 and OA-2) is a summing amplifier having a gain of 45. The capacitor in the

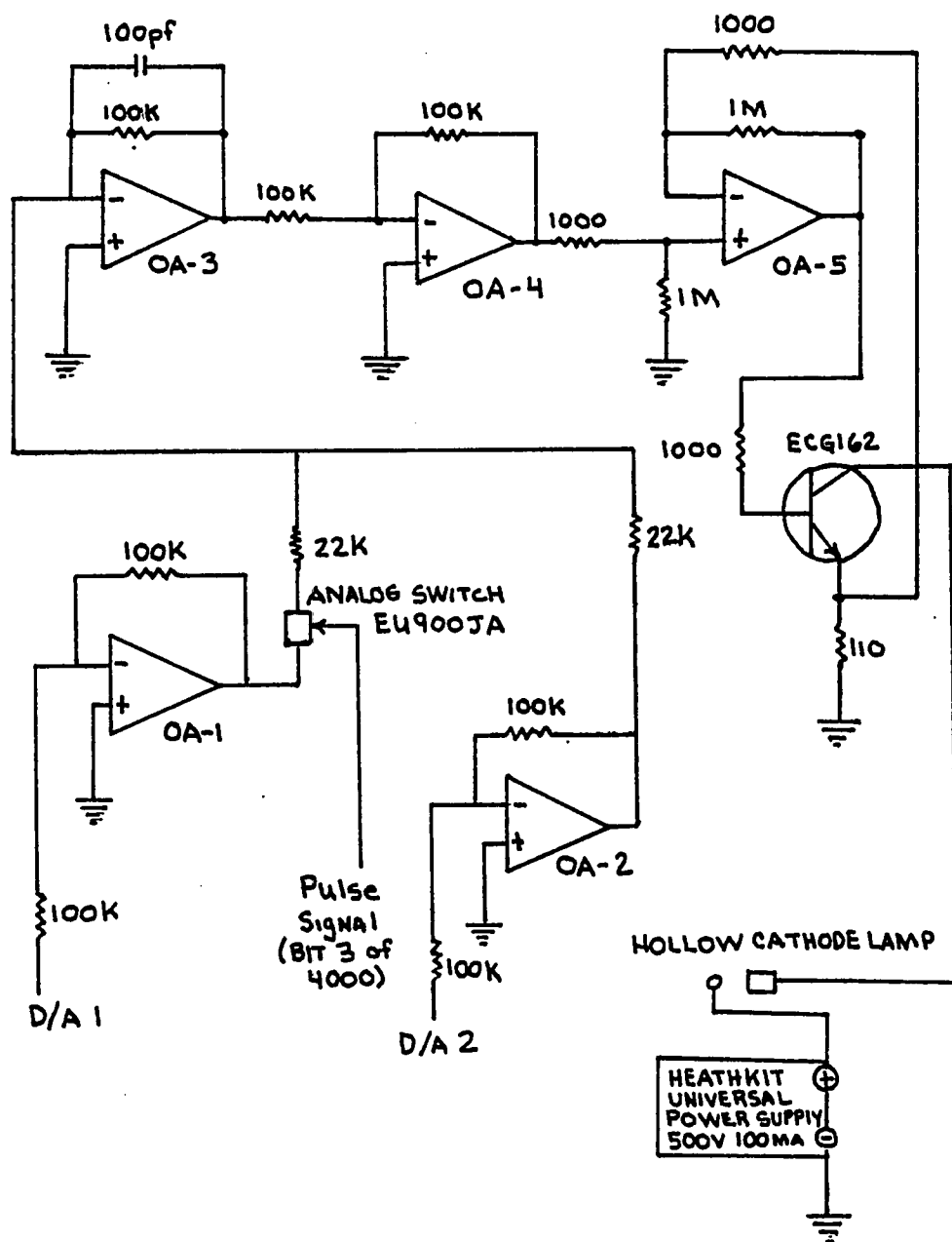


Figure 3. Schematic diagram for the hollow cathode lamp power supply. All operational amplifiers shown are Sylvania ECG 941D.

negative feedback loop allows this amplifier to also serve as a low pass filter with a time constant of 10 microseconds. The output of this amplifier is supplied to the input of an inverting amplifier (OA-4). The output of this amplifier is then connected to the input of a differential amplifier (OA-5) whose output is supplied through a resistor to the base of the regulator transistor. The emitter of the transistor is connected in parallel through resistors to ground and to the negative input of the differential amplifier (OA-5). As the current through the hollow cathode lamp increases, so too does the positive voltage supplied to the negative input of the differential amplifier. The output of the amplifier in response to this becomes less positive, thereby reducing the current allowed to pass through the transistor and the lamp. Likewise, if the lamp current becomes smaller, the output of the amplifier becomes more positive causing an increase in the current passed through the transistor and the lamp. Variations in the voltage output of the differential amplifier will compensate for small changes in the lamp current.

Detector for Phasing of Chopper

The schematic diagram for the detector which monitors the opening and closing of the chopper is shown in Figure 4. An infrared phototransistor TIL414 is placed inside a cylindrical tube which allows light to enter one end through a pin hole. The phototransistor and its housing are placed on the opposite side of the chopper from a small light source. When the chopper opens the phototransistor detects the light from this source at its base causing the current output from

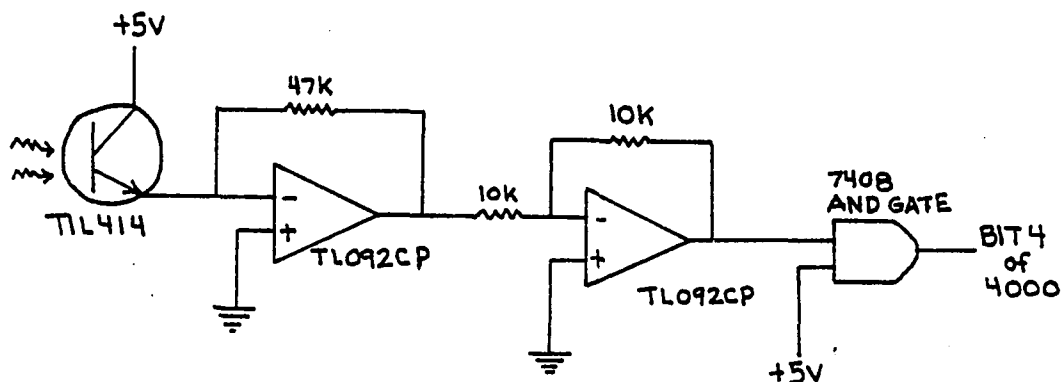


Figure 4. Schematic diagram of the IR transistor detector for phasing of chopper.

its emitter to increase from 25 nanoamps to several milliamps. The emitter current is supplied to a current-to-voltage converter whose gain is such that its maximum voltage output is -5 volts. This voltage is made positive by a unity gain inverter and then supplied to one input of a two input 7408 AND gate. The other input of the gate is supplied with +5 volts. When the chopper opens the output of the gate changes from 0 to +5 volts. This conversion is monitored by the microprocessor through the connection of the gate's output to bit 4 of \$4000.

The major advantage of the infrared phototransistor lies in its fast response times which are nominally 6 to 8 microseconds. Fast response is critical for accurately timing the pulsing of the hollow cathode lamp.

Amplification of the Signal from the PMT

The schematic diagram of the circuit for amplifying the signal from the PMT is shown in Figure 5. The microamp current from the PMT

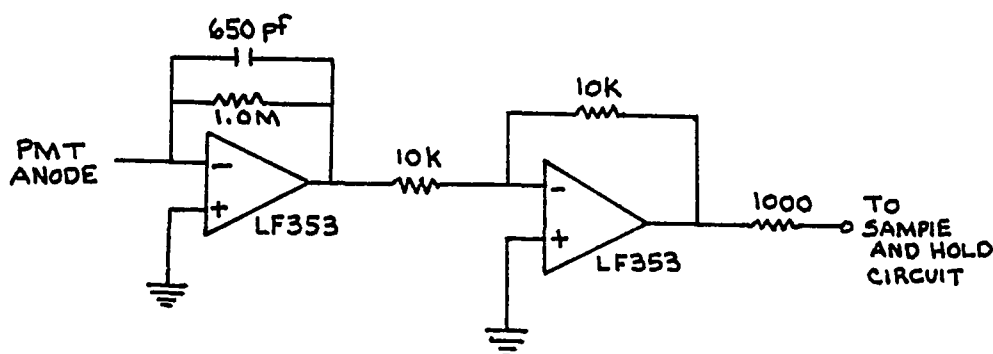


Figure 5. Amplifier circuit for the current signal from the photomultiplier tube.

is supplied to the negative input of a very high input impedance (10^{12}) National Semiconductor 353 FET opamp which is in the current-to-voltage converter configuration. The gain on the converter is 10^6 . A 650 picofarad capacitor is placed parallel to the feedback resistor to develop a low pass filter with a time constant of 650 microseconds. The output of the converter is made positive by a unity gain inverter whose output is supplied to the sample-and-hold circuit of the A/D converter. The amplifier is placed in a shielded chassis and well grounded. Connections made between the PMT and the amplifier are made through shielded coaxial cables.

Analog to Digital Conversion

The common methods of A/D conversion are the flash, the voltage-to-frequency, the single-slope, and dual-slope, the charge balancing, the sample-and-hold, and the pulse counting methods. The emission signal from the lamp and the flame can be extremely noisy due to flame flicker. Because of this, the voltage-to-frequency, single-slope, and the charge balancing methods are inappropriate. Of the four remaining

techniques the sample-and hold method was chosen for its simplicity, accuracy, and availability.

The schematic diagram of the sample-and-hold circuit is depicted in Figure 6. The voltage from the PMT signal amplifier is supplied through a FET analog switch (I) to the negative input of an inverter (OA-1) having a gain of 1.33. The output of the inverter is connected in parallel to the positive input of a follower amplifier (OA-2), to an analog switch (II) which connects to ground, and to a 0.1 microfarad low leakage capacitor. The voltage output of the follower is positive and is supplied to the negative input of a comparator (OA-3). Also connected to the negative input of the comparator (OA-3) is the negative voltage output of a 10-bit D/A converter. The positive input of the comparator (OA-3) is connected to ground. The output of the comparator is connected to the base of a Sylvania ECG289A fast switching transistor and also to a fast switching diode which connects to ground. The emitter of the transistor is connected to ground and its collector to a +5 volt power supply (through a 1500 ohm load resistor) and, also to bit 4 of \$4000.

When analog switches I and II are closed and opened, respectively, the 0.1 microfarad capacitor (connected to the positive input of OA-2) is allowed to follow the voltage of the unknown. When analog switch I is opened the capacitor is held at the voltage just prior to its opening. During this hold period the successive approximation routine takes place to determine a representative digital value for the voltage. After completion of this routine, analog switch II is closed and the capacitor discharged. In anticipation of obtaining

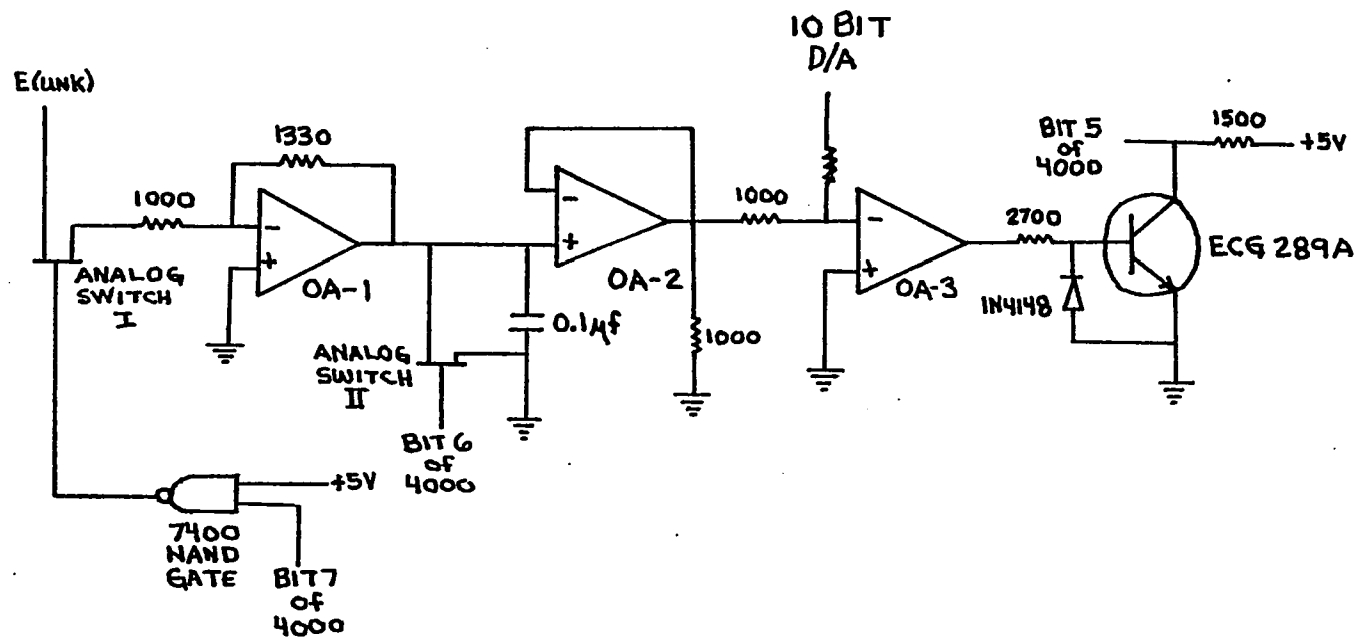


Figure 6. Sample and hold circuit. All operational amplifiers are National Semiconductor LF 353N.

the next value analog switch I is closed and analog switch II opened.

When the positive output voltage of the follower is greater in magnitude than the negative reference voltage of the D/A converter, the voltage supplied to the negative input of the comparator is positive. This results in the comparator output becoming negative. The negative voltage is passed to ground through the switching diode. As a result, the base of the transistor is unaffected and the signal to the PIA remains at +5 volts.

When the opposite condition exists, e.g., the magnitude of the negative voltage from the D/A converter is greater than the positive voltage from the follower, the comparator output is positive and the transistor is allowed to pass current. The signal to the PIA under these conditions is zero volts.

CHAPTER V

SOFTWARE DEVELOPMENT - 6800 MACHINE LANGUAGE

The flowcharts for the machine language software routines can be found in Appendix A and the programs in Appendix C.

The Main Machine Language Routine

The machine language routine begins at \$0C00. The first objective of this routine is to initialize the two peripheral interface adapters, PIA 1 and PIA 2. Ports A and B of PIA 1 have assigned addresses \$8000 and \$8002, respectively. Ports A and B of PIA 2 have assigned addresses \$4000 and \$4002, respectively. Ports \$8000, \$8002, and \$4002 have all of their bits assigned as outputs. Whereas, port \$4000 has its bits assigned as described in Table 1.

After initialization the peak and steady current values are set by storing the values in \$0CB1 and \$0CB2 into ports \$8000 and \$4002, respectively. The values in \$0CB1 and \$0CB2 originated from a user input during the Tiny Basic routine.

The next sequence of steps initializes the conditions required for pulsing the lamp and the acquisition of a data point. First, the initial conditions necessary for successive approximation are set. Next, in order to insure that the lamp is pulsed during the opening of the chopper, two wait routines are completed.

Once the initial conditions are set, the hollow cathode lamp is turned on to its peak current and the capacitor of the sample-and-

Table 1
Bit Assignment of Port \$4000 of PIA 2

<u>Bit</u>	<u>Hex value</u>	<u>Function</u>
1	1	2nd MSB to D/A 3
2	2	MSB to D/A 3
3	4	Signal to turn lamp on (0 V) or off (5 V)
4	8	Signal from chopper detector open (5 V) closed (0 V)
5	10	Signal from A/D ref. smaller (0 V) unk. smaller (5 V)
6	20	Signal to discharge capacitor discharge (5 V) disconnect (0 V)
7	40	Signal to allow charg- ing of capacitor charge (5 V) discharge (0 V)
8	80	not used

hold circuit is connected so that it can be charged by the signal from the PMT signal amplifier. After a set sample time the capacitor is disconnected from the amplifier and the hollow cathode lamp is returned to the steady current. The digital value representative of the voltage held by the capacitor is evaluated by a successive approximation routine. Once the routine is completed the digital value is stored and the capacitor discharged.

The next sequence of steps accomplishes the acquisition of another digital value that is representative of the emission from the flame and background noise. The steps involved are exactly the same as those previously described, however, the wait routines insure that the chopper is closed and hollow cathode lamp is left at the steady current.

Once the digital value of the emission intensity is obtained, the preset value on \$OCB3, which is the number of sets of data points to be taken, is decremented by one. As long as the value in \$OCB3 does not equal zero another set of data points is obtained and stored. Once all of the sets of data points have been taken, average values of each data type is calculated through a sequence of addition and division subroutines. The average "peak" value is stored in the extended location \$OCE3-\$OCE4 and the average "emission" value in the extended location \$OCE5-\$OCE6.

Before returning to basic all of the conditions necessary for repeating the routine are reset.

Initialization Subroutine

This subroutine (\$OCC1-\$OCD0) initializes the conditions necessary for the successful completion of data acquisition by successive approximation.

Wait for the Chopper to Open Subroutine

This subroutine (\$OCA7-\$OCB0) detects the opening of the chopper. The signal from the amplifier to the infrared transistor detector is

received at bit 4 of \$4000. When this bit is set the chopper is open. To detect this condition the value in \$4000 is "anded" to, and the result compared to the value \$08. If the result and "anding" and \$08 are equal then the chopper is open. If the chopper is closed the routine loops back to obtain a new value from \$4000 and repeats the comparison procedure. The routine keeps looping back until the chopper is found to be open.

Wait for the Chopper to Close Subroutine

This subroutine (\$0C9D-\$0CA6) is essentially the same as that for the detection of the opening of the chopper except this routine keeps looping back until the chopper is found to be closed.

Data Acquisition Subroutine

This subroutine (\$0CE9-\$0D55) consecutively sets each bit of a ten bit value that controls the voltage output of a D/A converter to determine the representative digital value for the unknown voltage held by the capacitor of the sample-and-hold circuit. The most significant bit (MSB) of the ten bit value is set first and the voltage produced by the D/A compared to the unknown. If the D/A voltage is less than the unknown, the bit value is retained. In a like manner the sum of the retained bit values and consecutively smaller new bit values are tested. The final sum of all the retained values is equivalent to the value representative of the unknown voltage.

Because each port of a PIA has only eight bits available for data output, two ports have to be used to obtain the ten bits required

to operate the D/A converter. The two most significant bits are taken from \$4000 and the remaining eight bits from \$8000. The values initially placed into \$4000 and \$8000 are \$03 and \$00, respectively. The voltage produced by the D/A for this combination is compared to the unknown voltage. If the D/A voltage is greater than the unknown voltage the value in \$4000 is decremented by one. Testing and decrementing continues until the D/A voltage is less than the unknown voltage or until the value in \$4000 is equal to zero. The final value in \$4000 is stored into \$0CB4.

Once the value in \$0CB4 has been obtained the next eight bits are tested. This is initialized by loading \$8000 with the value in \$0CB5, which is initially \$80, and loading \$4000 with the value in \$0CB4. If the voltage produced by this combination is less than the unknown voltage then the value on \$0CB5 is added to the value in \$0CB6, whose value is initially equal to zero. If the D/A voltage is greater than the unknown voltage the addition is not made and the routine proceeds directly to the next step which is the division of the value in \$0CB5 by two. The resultant value in \$0CB5 is summed with the value in \$0CB6 to produce the next value to be loaded into \$8000 and tested. The rest of the eight bits are tested in a like manner and the final value in \$0CB6 when combined with the value in \$0CB4 represents the digital value for the unknown.

Store Data Point Subroutine

This subroutine is located between addresses \$0E27 and \$0E33. The value in \$0CB4 is the most significant byte and the value in \$0CB6

the least significant byte of the data value to be stored. Previous to this subroutine the index register is loaded with the location where the data value is to be stored. The least significant byte is stored first followed by the most significant byte.

Addition Subroutine

Before this subroutine (\$0D9C-\$0DB3) can be entered the value of the location where the most significant byte of the last data value taken is stored must be loaded into the index register. The MSB is loaded into accumulator A and the LSB into accumulator B. The MSB of the next data value is added to the contents of accumulator A and the LSB to accumulator B. If, upon addition of the LSB, the carry is set then the value in accumulator A is incremented by one. The process continues until the last data value has been added. The sum of the data values is retained in the accumulators when this subroutine returns to the main program.

Division Subroutine

The first part of this subroutine (\$0DB4-\$0DF6) determines the number of data values that were taken. This quantity is given by the value in \$0CDE and can have the possible decimal values of 2, 4, 8, 16, 32, or 64. The value in \$0CDE is first compared to the value 2. If they are not equal then the latter is multiplied by two until they are. The value in \$0CDD, which is initially equal to \$01, is incremented by one each time a multiplication by two occurs. The final value of \$0CDD is the number of times the sum obtained from the addition

subroutine has to be divided by two.

The LSB of the sum is divided first. This is accomplished by rotating the LSB (\$OCD6) to the right as many times as specified by the value in \$OCDD. With each rotation, the carry is cleared so that the bit values are not recycled. The division of the MSB requires the retention of all of its bit values. This is accomplished by rotating the value of the MSB (\$OCD7) to the right into the carry and then rotating the carry into a previously cleared location, \$OCD1. Again the number of rotations is determined by the value in \$OCDD. The remaining value in \$OCD7 is the average MSB. The average LSB is obtained by adding the values in \$OCD1 and \$OCD6 and storing the result in \$OCD6.

CHAPTER VI

SOFTWARE DEVELOPMENT - HEATHKIT TINY BASIC

A major goal in the software development was to obtain the percent absorption (%A) and emission data without causing a significant interruption in the pulsing of the hollow cathode lamp which could result in instability of the lamp. For this reason the data is obtained continuously by means of a closed loop software routine and calculations are kept to a minimum.

The flowcharts for the Tiny Basic routines are found in Appendix B and the program in Appendix D.

Tiny Basic Main Routine

The first objective of the routine is to have the user input the values of the peak and steady currents that are to be used to operate the hollow cathode lamp. The values to be input are of inverse logic with 0 representing the maximum and 255 the minimum currents. Once the peak and steady currents are selected the user is notified to aspirate the blank solution. Five sets of data are taken initially to allow time for the aspiration rate to steady. The data printed out for the user, however, is not used in any calculations. After completing this, another five sets are taken whose values are used in the calculation of %A and emission. The variables L and M represent the sums of the maximum and minimum intensity values, respectively.

Once the five sets of data and L and M have been obtained, the user is notified to aspirate the sample.

Since data cannot be obtained for the blank and the sample at the same time, the values of L and M are assumed to remain constant for the period of time it takes to aspirate the sample. This assumption is not a good one when the monitored emission signal is very noisy, therefore, it is advantageous to calculate the %A and the emission values for each set of data taken. Five sets of data are obtained, after which, the routine loops back to obtain updated values of L and M for another blank. It should be noted that usually only the last three of the five %A values obtained for the sample are useful since the first two are taken during the period of initial aspiration.

%A and Emission Calculation

The theoretical considerations for the calculation of %A and emission were given in Chapter IV. The values of B and D in the Data Acquisition Subroutine are those of the maximum and minimum emission intensities, respectively. The subroutine obtains two sets of these values. The sum of the values of B is given by F and the sum of the values of D by G. For the blank the subroutine is repeated five times and the difference G-F is calculated for each of the five. The sum of these differences is given by L. In a like manner, M represents the sum of the five values of G. The calculation of %A for the sample involves multiplying the quantity G-F by five, dividing by the value of L, and then subtracting the result from 10000. The emission value

is obtained by taking the difference between M and five times G.

$$\%A = 10000 - (5 \times (G - F) / L) \quad (18)$$

$$\text{Emission} = M - (5 \times G) \quad (19)$$

Data Acquisition Subroutine

This subroutine obtains two values, F and G, representative of the sum of the two maxima (B) and two minima (D) intensity values, respectively.

Initially the variables F and G are set equal to zero and E equal to two. The value E determines the number of individual values to be summed. If its value of changed so too must the method of calculation of %A and emission. The individual values for the maximum and minimum intensities are "Peeked" from the extended memory locations 3299-3300 and 3301-3302, respectively. To convert these values to their decimal equivalent, the values in the most significant bytes are multiplied by 256 and then added to the values in their respective least significant bytes. Before returning to the main routine the values of F and G are printed out for the user to observe.

CHAPTER VII

RESULTS AND CONCLUSIONS

The operation of the microprocessor controlled pulsed hollow cathode lamp system is relatively simple. The first step is to select the peak and steady current values. The peak value can be obtained by using the following equation

$$\text{Peak Value} = \frac{\text{Peak current (ma)} - 81.76}{-0.2757} \quad (20)$$

where 81.76 and -0.2757 are the intercept and slope, respectively, determined from a plot of peak current (ordinate) vs. peak value (abscissa). This equation is applicable when a steady current of 1.5 milliamps (ma) (steady current value = 250) is used. It is necessary in the selection of the peak and steady currents to maintain a time averaged current that is less than the continuous current specified by the manufacturer of the lamp. The time averaged current can be calculated through the use of the following equation.

$$\text{Time Averaged Current (ma)} = 0.1126 \text{ Peak Current (ma)} + 0.8874 \text{ Steady Current (ma)} \quad (21)$$

If the time averaged current is greater than the continuous current the life of the lamp will be reduced.

Table 2 shows the effect of increasing the peak current and, therefore, the lamp intensity on the slopes of the calibration curves (ordinate - ma; abscissa - ppm) for cobalt, nickel, and copper. As the peak current is increased the value of the slope becomes smaller

Table 2

Effect of Increased Emission from the Pulsed
Hollow Cathode Lamp on Cobalt, Nickel, and
Copper Calibration Curves
(ordinate - ma; abscissa - ppm)

<u>Element</u>	<u>Peak Current (ma)</u>			
	<u>80(00/250)*</u>	<u>74(30/250)*</u>	<u>64(60/250)*</u>	<u>58(90/250)*</u>
<u>Cobalt</u>				
slope	0.0158	0.0170	0.0190	0.0217
intercept	0.00708	0.00310	0.000291	-0.00134
correlation	0.998	0.999	0.999	0.998
conditions	dynode voltage 900 VDC; acetylene 9/ air 10; slit width 100 microns; wavelength 2407.5 angstroms; concentrations 2.0, 4.0, 6.0, 8.0, 10 ppm.			
<u>Nickel</u>				
slope	0.0227	0.0302		
intercept	0.00131	-0.0107		
correlation	0.996	0.994		
conditions	dynode voltage 900 VDC; acetylene 10/ air 10; slit width 100 microns; wavelength 2320.9 angstroms; concentrations 2.0, 4.0, 6.0, 8.0, 10 ppm.			
<u>Copper</u>				
slope	0.0208	0.0220	0.0259	0.0308
intercept	-0.0221	-0.0267	-0.0366	-0.0461
correlation	0.993	0.993	0.990	0.995
conditions	dynode voltage 740 VDC; acetylene 9/ air 10; slit width 100 microns; wavelength 3247.5 angstroms; concentrations 2.0, 4.0, 6.0, 8.0, 10 ppm.			

* present values (peak/idle)

for all the curves. This decrease in the slope indicates a decrease in
sensitivity which is probably due to the enhancement of line reversal

and broadening at the higher lamp intensities.

Once the peak and steady currents have been selected it is necessary to have a warmup period for the lamp so that thermal equilibrium can be obtained. The single element lamps of copper (Westinghouse WL22606, Ar filled) and silver (Westinghouse WL22806, Ar filled) were each found to reach equilibrium rapidly and produced extremely steady emission outputs. The multielement lamp which contained cobalt, chromium, and nickel (Westinghouse WL23174, Ne filled) on the other hand never reached a steady emission output, especially for chromium. However a condition was reached where the rate of increase in the intensity was slow enough that there was no significant difference between the intensity measured before and after the period of sample aspiration. The plots relating the emission intensities produced by varying the PMT dynode voltage and their relative standard deviations are given in Appendix G.

After the warmup period the blank and sample can be aspirated. This time period is indicated to the user by the display on the CRT. Five sets of %A and emission values are obtained for each sample. The first two sets are, generally, useless due to the initial aspiration interferences. However, aspiration of the sample can be made as many as ten times each minute.

Because the gain on the PMT amplifier is not high enough to measure emission of the analyte at the same time as the %A, its value is generally equal to zero during absorbance measurements. To obtain the emission values of the analyte, the hollow cathode lamp should be left off by loading the value 255 into the microprocessor for both the

peak and steady currents. Table 3 gives the regression analysis results for the emission of copper and calcium standards.

Table 3

Regression Analysis of Emission Calibration
Curves for Copper and Calcium
(ordinate - intensity; abscissa - ppm)

<u>Characteristic</u>	<u>Copper</u>	<u>Calcium</u>	<u>Calcium*</u>
slope	0.341	2.87	0.0716
intercept	151	574	28.2
standard deviation y	17.5	104	4.24
standard deviation slope	0.0139	0.0519	0.00212
standard deviation intercept	9.19	34.4	1.40
correlation	0.985	0.992	0.980
based on a data, a =	50	50	50
concentrations 200, 400, 600, 800, 1000 ppm			
dynode voltage	1200	1200	940
acetylene	9	9.5	9.5
air	10	9.5	9.5
slit width (microns)	100	150	100
wavelength (angstroms)	3247.0	4226.7	4226.7

*Data obtained from use of Jarrell-Ash AA/AE Spectrometer.

The major disadvantage of the system is that the fixed gain on the PMT amplifier, which is nominally set for absorbance studies, requires the use of much higher dynode voltages on the PMT for emission studies. The high dynode voltages cause instabilities in the PMT output due to space charge effects. A possible solution to this problem is to provide the PMT amplifier with variable gain. The %A value would be obtained from the intensities measured for the blank and sample at low gain on the amplifier. The emission values would be obtained from intensities measured when the chopper is closed and the amplifier is at high gain. A major objective would be to make sure

that at no time will the PMT be exposed to a lamp pulse when the amplifier is at the high gain which could result in saturation of both the PMT and the amplifier.

Table 4 shows the results of the linear least squares regression analysis for the calibration curves for copper and cobalt. The concentration range analyzed was between 2 and 10 parts per million (ppm) and the correlation constants obtained were of the order of 0.99.

Table 4

Regression Analysis of Calibration Curves for Copper and
Cobalt Using Pulsed A.A.
(ordinate - A; abscissa - ppm)

<u>Characteristic</u>	<u>Copper</u>	<u>Cobalt</u>
slope	0.0222	0.0123
intercept	-0.0313	0.00628
standard deviation y	0.00959	0.00293
standard deviation slope	0.000480	0.000146
standard deviation intercept	0.00318	0.000971
correlation	0.989	0.997
based on a data, a =	50	50
concentrations 2.0, 4.0, 6.0, 8.0, 10 ppm		
dynode voltage	720	900
acetylene	9	10
air	10	9
slit width (microns)	100	100
wavelength (angstroms)	3247.5	2408.0
peak current (milliamp)	74 (30/250)	74 (30/250)

Tables 5 through 7 compare the calibration curves obtained using pulsed A.A. and regular A.A. methods for the determination of chromium, nickel, and silver. The slopes of these curves again indicate a decrease in sensitivity at the higher lamp emission intensities. The correlation for both the pulsed and regular curves are of the order of 0.99 indicating similar linear response over the range of concentrations analyzed. Though the detection limit was not determined it is

Table 5

Regression Analysis of Calibration Curves for Chromium
Regular and Pulsed A.A.
(ordinate - A; abscissa - ppm)

<u>Characteristic</u>	<u>Regular</u>	<u>Pulsed</u>
slope	0.0162	0.00989
intercept	0.00212	0.00400
standard deviation y	0.00432	0.00381
standard deviation slope	0.000216	0.000190
standard deviation intercept	0.00143	0.00126
correlation	0.996	0.991
concentrations 2.0, 4.0, 6.0, 8.0, 10 ppm		
based on a data, a =	50	50
dynode voltage	720	720
acetylene	13	13
air	10	10
slit width (microns)	100	100
wavelength (angstroms)	3578.7	3578.7
peak current (ma)	--	74 (30/250)
cont. current (ma)	25	--

Table 6

Regression Analysis of Calibration Curves for Nickel
Regular and Pulsed A.A.
(ordinate - A; abscissa - ppm)

<u>Characteristic</u>	<u>Regular</u>	<u>Pulsed</u>
slope	0.00784	0.0240
intercept	0.00342	-0.0293
standard deviation y	0.00313	0.00956
standard deviation slope	0.000156	0.000478
standard deviation intercept	0.00104	0.00317
correlation	0.991	0.991
based on a data, a =	50	50
concentrations 2.0, 4.0, 6.0, 8.0, 10 ppm		
dynode voltage	940	940
acetylene	9.5	9.5
air	10	10
slit width (microns)	150	150
wavelength (angstroms)	2320.0	2320.0
peak current (ma)	--	80 (00/250)
cont. current (ma)	25	--

Table 7

Regression Analysis of Calibration Curves for Silver
 Regular and Pulsed A.A.
 (ordinate - A; abscissa - ppm)

<u>Characteristic</u>	<u>Regular</u>	<u>Pulsed</u>
slope	0.0135	0.00943
intercept	0.00131	-0.000780
standard deviation y	0.00403	0.00264
standard deviation slope	0.000202	0.000132
standard deviation intercept	0.00134	0.000875
correlation	0.995	0.995
based on a data, a =	50	50
concentrations 2.0, 4.0, 6.0, 8.0, 10 ppm		
dynode voltage	740	740
acetylene	9.5	9.5
air	10	10
slit width (microns)	100	100
wavelength (angstroms)	3280.7	3280.7
peak current (ma)	--	74 (30/250)
cont. current (ma)	30	--

felt that a lower limit would be obtained with the pulsed method due to the increased emission intensity from the lamp causing more efficient absorption.

The linear least squares regression analysis for each element is based on 50 data values, ten for each concentration. Each of these values is an average of 128 making a total of 6400 individual determinations.. For the regression analysis to be more representative of the data all 6400 should be used, however, since memory was limited, this was not possible,

Because the microprocessor serves many functions, such as pulsing the lamp. data acquisition, and various calculations, it is difficult to pulse the lamp at a constant frequency. As a result, instabilities

in the emission intensity output of the lamp may occur. For this reason, it would be advantageous to pulse the lamp by use of a separate circuit and to use the microprocessor for data acquisition and peak and steady current control. The circuit could be designed so that the microprocessor could also regulate the various pulsing parameters such as peak width and pulsing frequency.

Determination of Chromium and Nickel in Steel

The standard addition method was used to determine the concentration of chromium and nickel in steel. The unknown used was a SAE TS8615 steel alloy. The standard used was a NBS 101f heat resisting steel alloy. Both unknown and standard were selected for their similar composition which alleviated problems that might have occurred due to spectral interferences. The steel samples were dissolved in aqua regia and diluted to concentrations with double distilled water. Double distilled water served as the blank. Five standard solutions were made ranging in composition from 2 to 10 parts per million (ppm) in chromium and 1.1 to 5.4 ppm in nickel. Each of the five solutions contained equivalent concentrations of unknown analyte elements. A 10 cm slot laminar flow burner was used to produce the air/acetylene flame into which the samples were aspirated.

The results of the analyses for chromium and nickel in the unknown and the operating conditions used are given in Tables 8 and 9.

Ten absorbance values were obtained for each of the five concentrations resulting in 50 data values being used in the regression analysis. The correlation coefficients for all of the trials are of

Table 8

Results and Regression Analysis of Standard Addition
Curves for Chromium in Steel by Pulsed A.A.
(ordinate - A; abscissa - ppm)

Characteristic	Trial 1	Trial 2	Trial 3
slope	0.00871	0.00687	0.00609
intercept	0.00977	0.00750	0.00670
standard deviation y	0.00356	0.00293	0.00241
standard deviation slope	0.000178	0.000147	0.000120
standard deviation intercept	0.00182	0.000972	0.000799
correlation	0.990	0.989	0.991
based on a data, a =	50	50	50
y = 0, x =	-1.12	-1.09	-1.10
concentrations 2.0, 4.0, 6.0, 8.0, 10 ppm			
dynode voltage	720	720	720
acetylene	13.5	13.5	13.5
air	10	10	10
slit width (microns)	100	100	100
wavelength (angstroms)	3578.7	3578.7	3578.7
peak current (ma)	80(00/250)	80(00/250)	80(00/250)
% by weight	0.550	0.546	0.550
RSD of % by weight	12.3	13.1	12.1
mean % by weight	0.549	RSD 12.4	
accepted value	0.57	precision 3.7%	

the order of 0.99. The relative standard deviation (RSD) in the percent by weight values were calculated by the propagation of errors from dividing the intercept by the slope. These RSD values are about twice the magnitude expected. This is likely due to a combination of flame flicker noise and poor fuel regulation to the burner. Nickel has a very weak emission line and any change in signal due to absorbance is small. As a result, slight noise will cause large relative changes in the absorbance value obtained. Likewise chromium requires a reducing flame with a well defined fuel ratio. Regulation can be extremely difficult and, therefore, absorbance values can vary with time. The RSD values might be reduced if the regression analysis

Table 9

Results and Regression Analysis of Standard Addition
Curves for Nickel in Steel by Pulsed A.A.
(ordinate - A; abscissa - ppm)

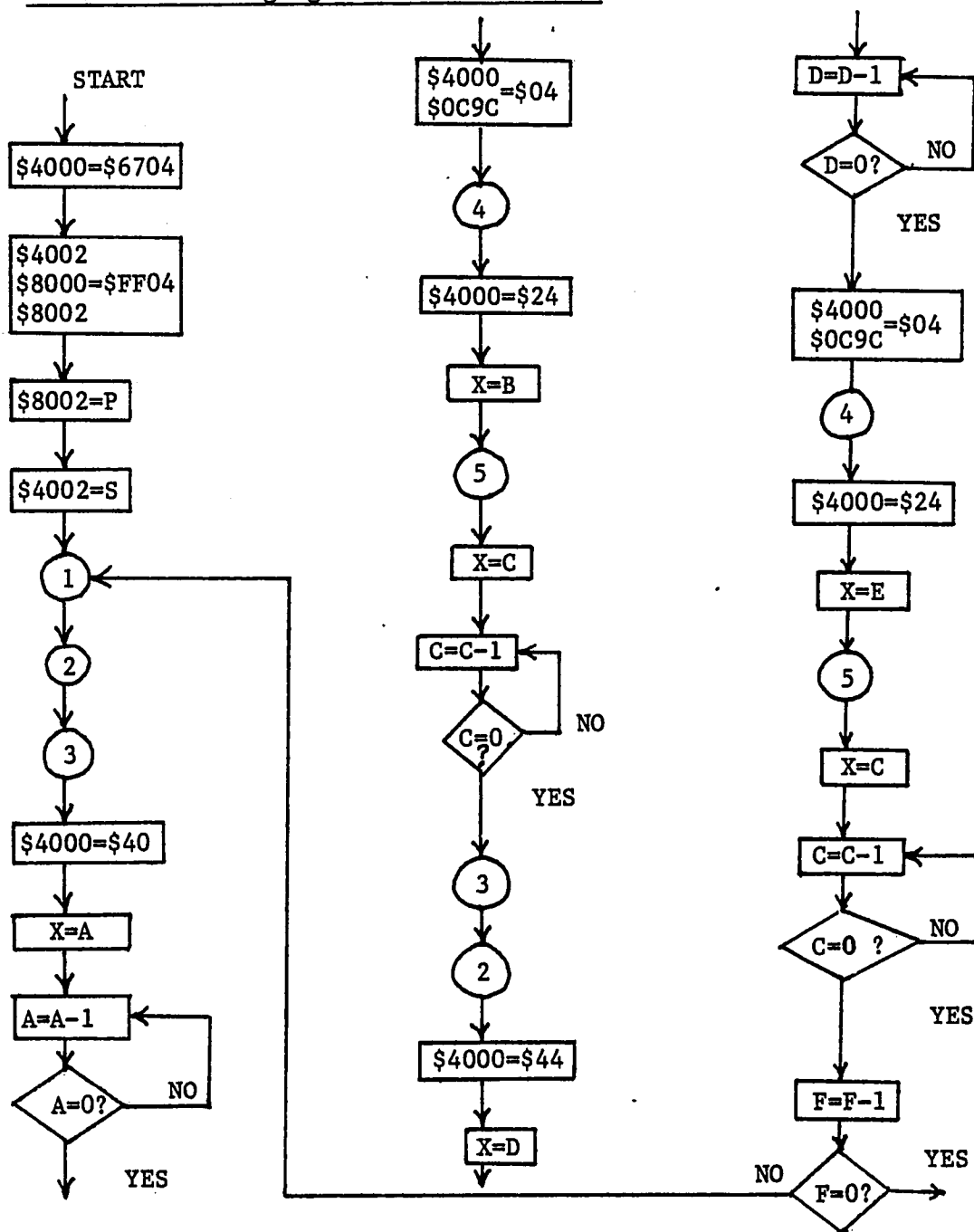
Characteristic	Trial 1	Trial 2	Trial 3
slope	0.0137	0.0125	0.0124
intercept	0.0133	0.0120	0.0107
standard deviation y	0.00330	0.00230	0.00255
standard deviation slope	0.000308	0.000215	0.000238
standard deviation intercept	0.00110	0.000768	0.000853
correlation	0.998	0.993	0.991
based on a data, a =	50	50	50
y = 0, x =	-0.968	-0.961	-0.865
concentrations 1.1, 2.2, 3.2, 4.3, 5.4 ppm			
dynode voltage	960	960	960
acetylene	10	10	10
air	10	10	10
slit width (microns)	150	150	150
wavelength (angstroms)	2320.0	2320.0	2320.0
peak current (ma)	80(00/250)	80(00/250)	80(00/250)
% by weight	0.474	0.481	0.432
RSD of % by weight	8.60	6.63	8.18
mean % by weight	0.462	RSD 7.79	
accepted value	0.49	precision 5.7%	

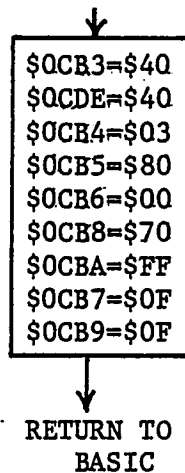
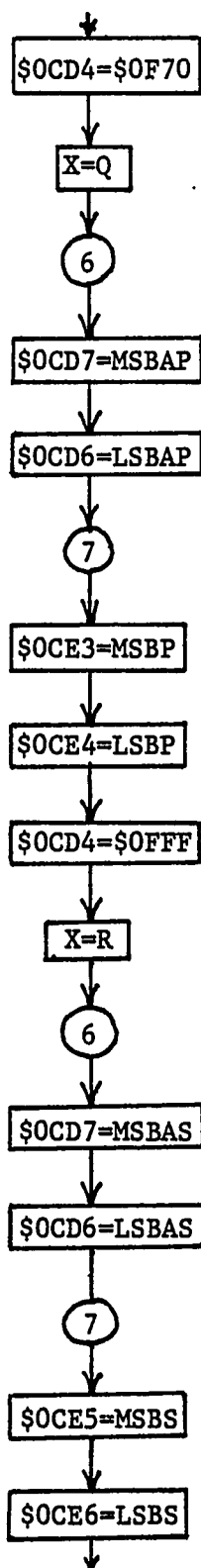
had reflected all of the 6400 individual determinations that were made instead of the 50 average values. Also, the use of a nitrous-oxide/acetylene flame would produce a much quieter signal and reduce spectral interferences that may have been present due to molecule species in the flame. The reproducibility of the A/D conversion is reflected in the plots of dynode voltage to the PMI versus the measured lamp intensity that are given in Appendix G. The RSD values are generally less than 0.5%. This error would not explain the large RSD values obtained for the percent by weight values.

APPENDIX A

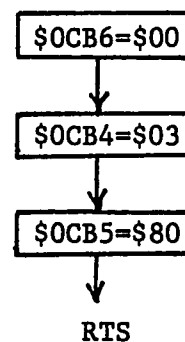
APPENDIX A

MACHINE LANGUAGE ROUTINE FLOWCHARTS

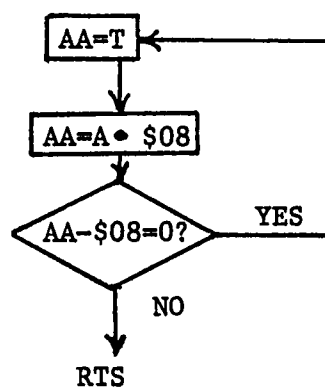
Main Machine Language Routine Flowchart

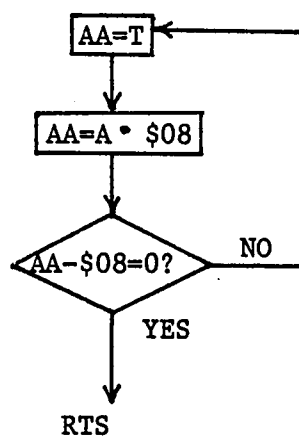
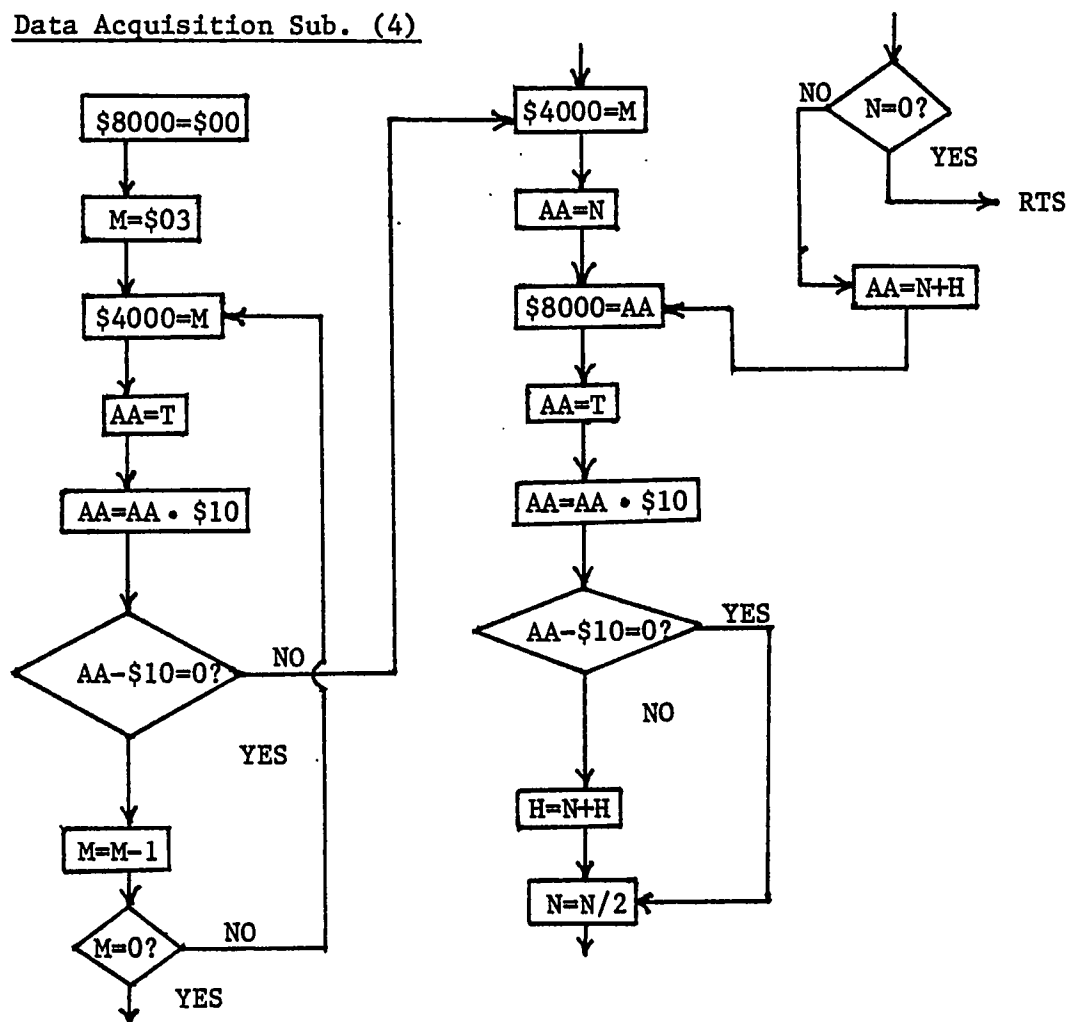


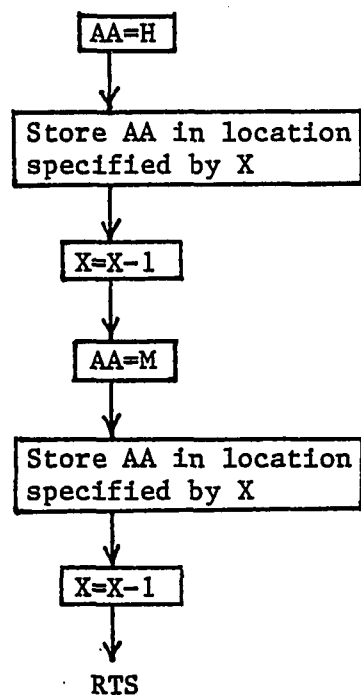
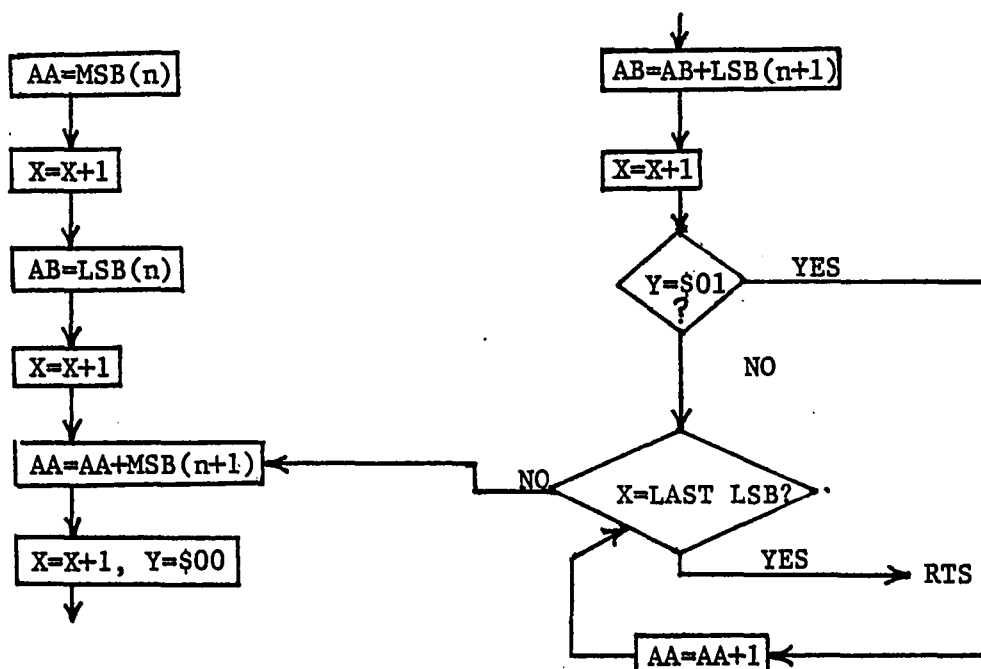
Initialization Subroutine (1)

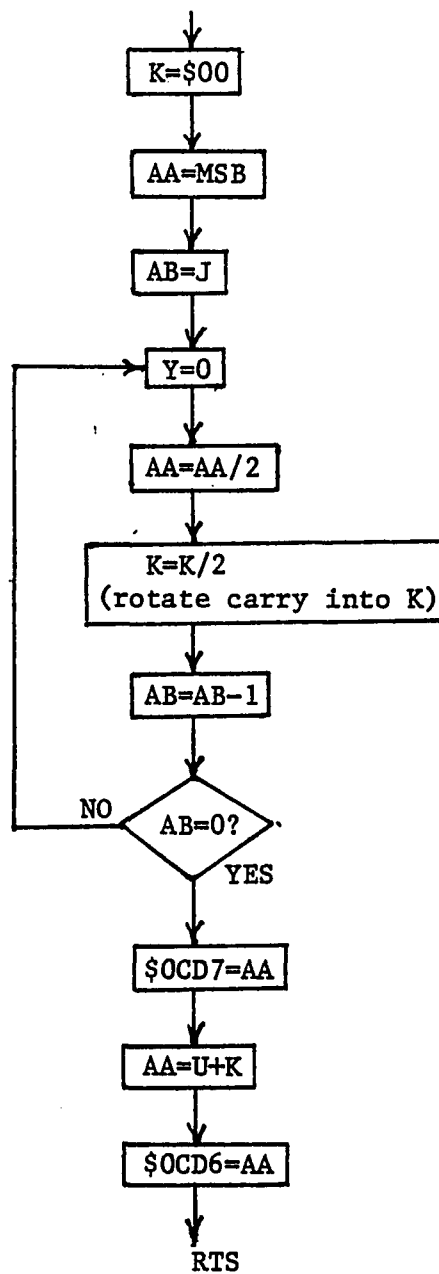
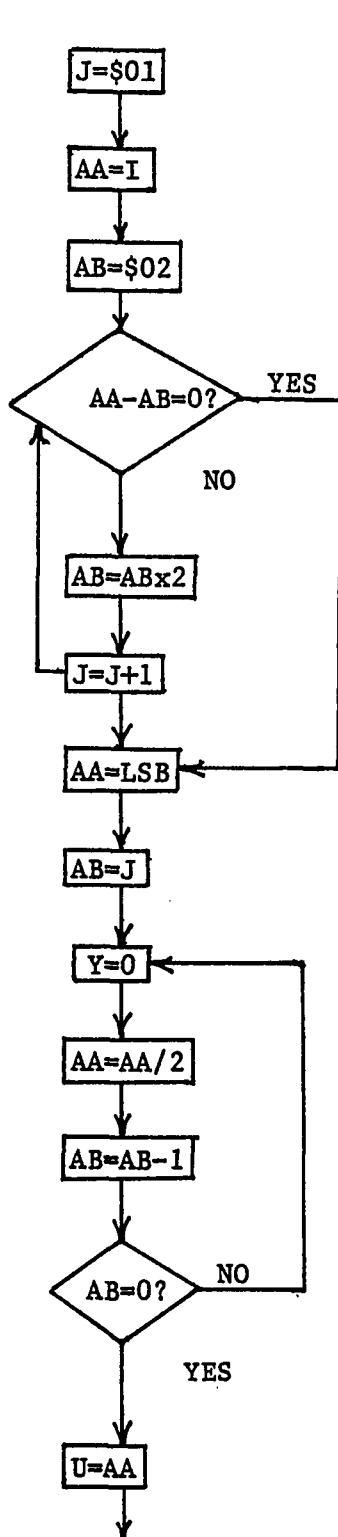


Wait for Chopper to Close Sub. (2)



Wait for Chopper to Open Sub. (3)Data Acquisition Sub. (4)

Store Data Sub. (5)Addition Sub. (6)

Division Sub. (7)

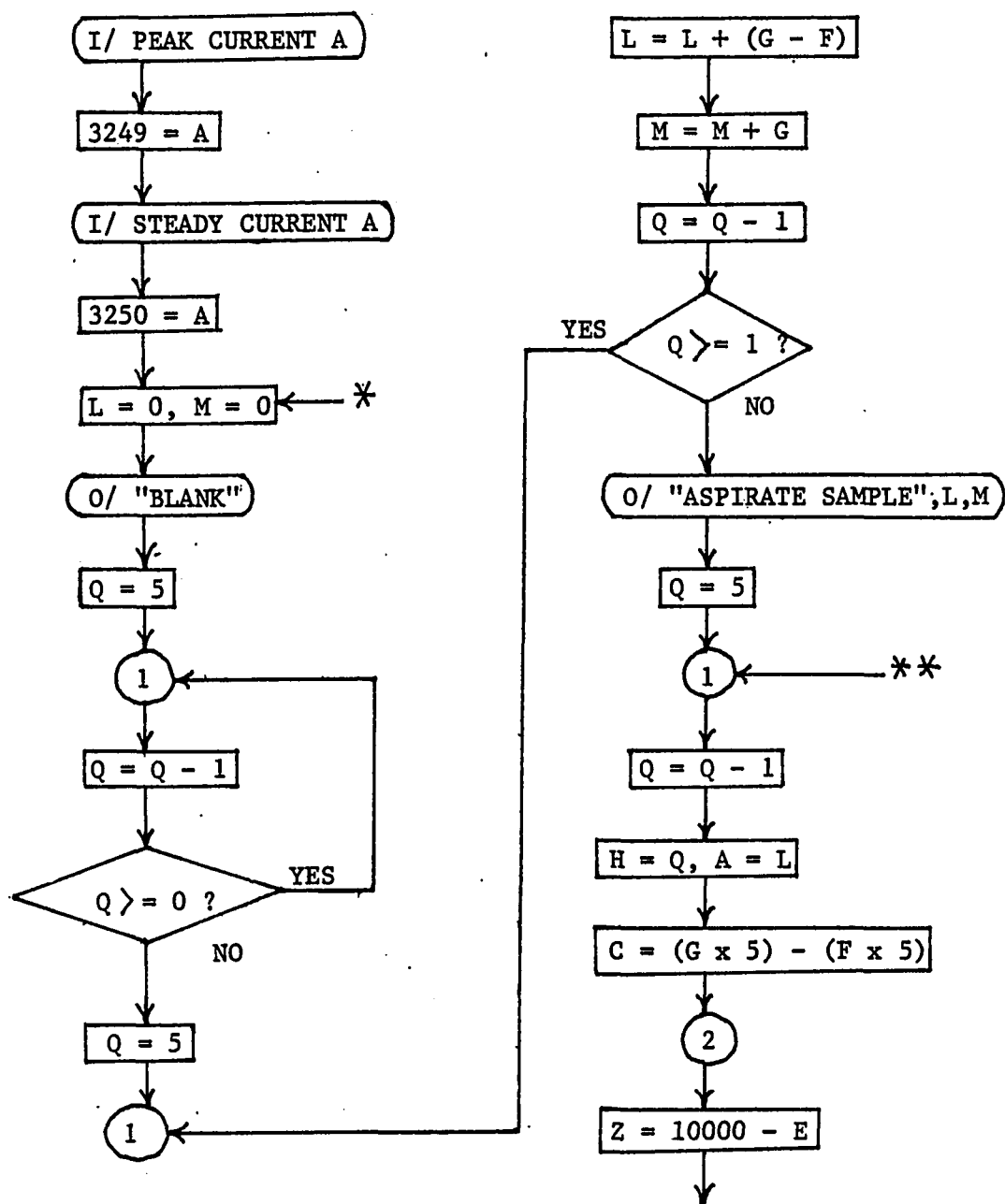
Term Symbols

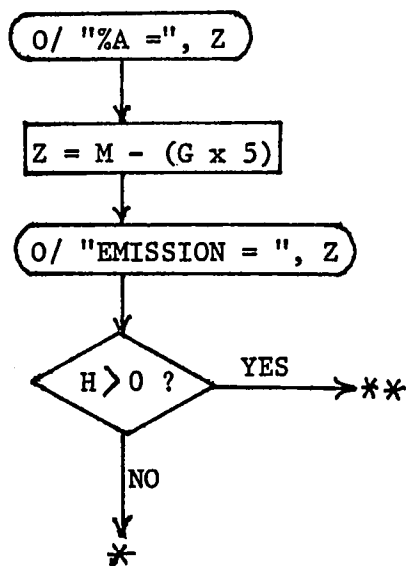
A	peak current value
B	location where to store peak data value
C	discharge time
D	sample time for steady data value acquisition
E	location where to store steady data value
F	#sets of data left to be obtained
H	value in \$OCB6 (initially = \$00)
I	quantity of data taken
J	value in \$OCDD
K	value in \$OCD1
M	value in \$OCB4 (initially = \$03)
N	value in \$OCB5 (initially = \$80)
P	peak current value
Q	location where MSB of last peak data value taken is stored
R	location where MSB of last steady data value taken is stored
S	steady current value
T	value in \$4000
U	value in \$OCD6
X	index register
Y	carry
AA	accumulator A
AB	accumulator B
MSBS	MSB of average steady value
LSBS	LSB of average steady value
MSBP	MSB of average peak value
LSBP	LSB of average peak value
MSBAS	MSB of sum of data for steady value
LSBAS	LSB of sum of data for steady value
MSBAP	MSB of sum of data for peak value
LSBAP	LSB of sum of data for peak value

APPENDIX B

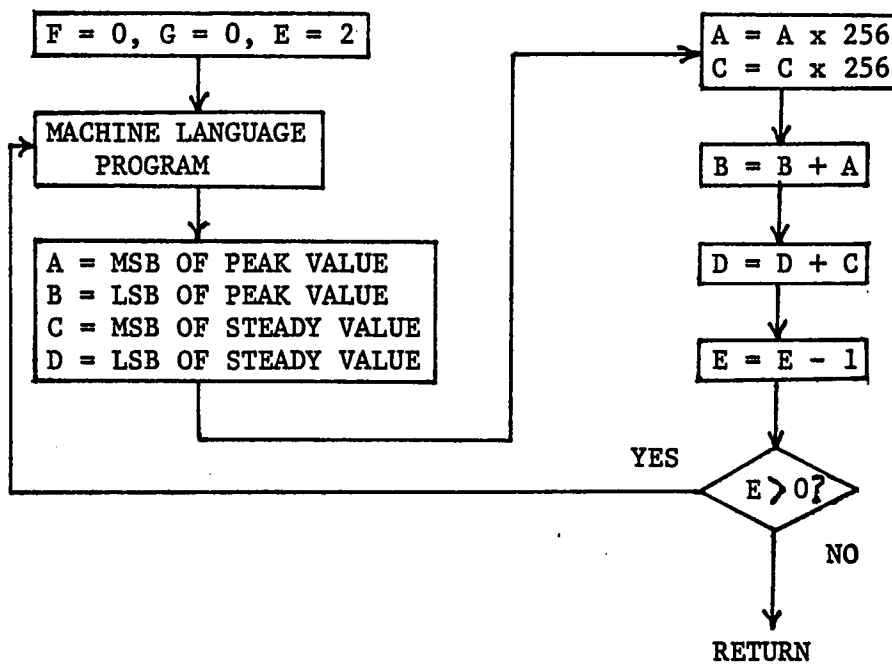
APPENDIX B

TINY BASIC ROUTINE FLOWCHARTS

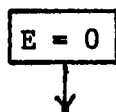
Main Routine

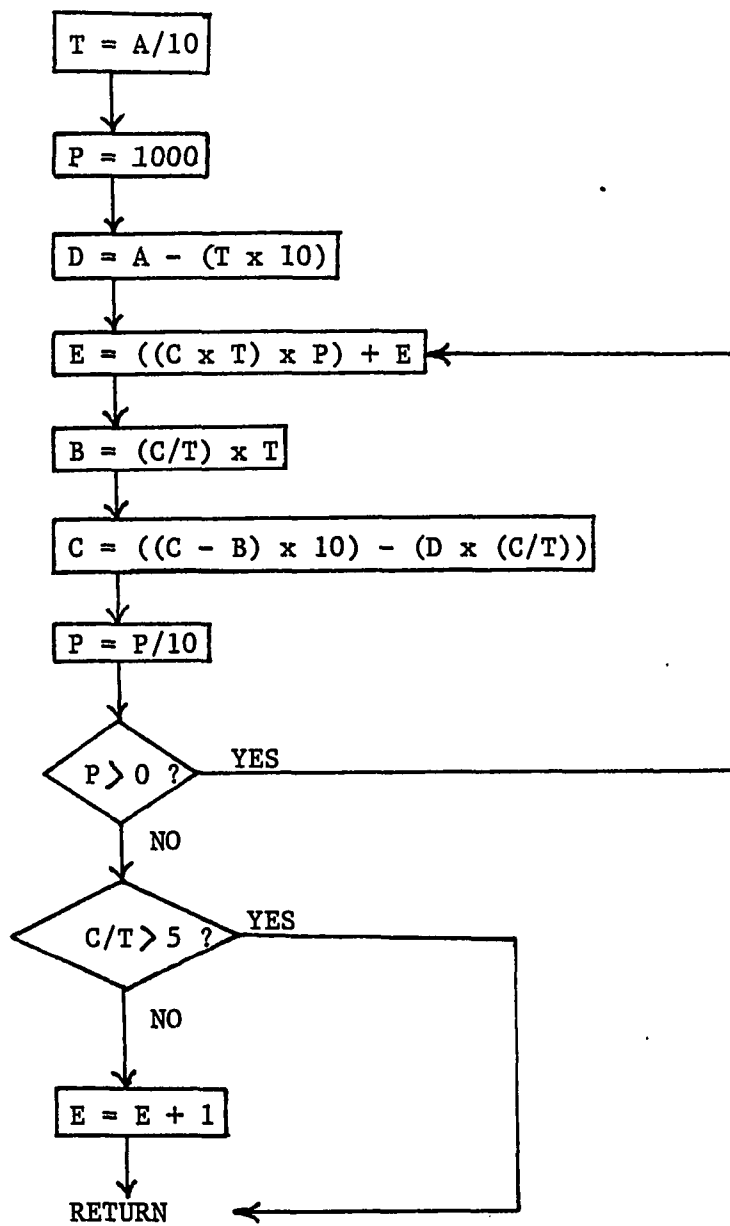


Data Acquisition Sub. (1)



Division Sub. (2)





APPENDIX C

APPENDIX C

MACHINE LANGUAGE PROGRAM

0C00	LDX	CE 6704	Initialize PIAs. Load index reg. with 6704 and store in 4000.
0C03	STX	FF 4000	
0C06	LDX	CE FF04	Load index reg. with FF04 and store in 4002, 8000, and 8002.
0C09	STX	FF 4002	
0C0C	STX	FF 8000	
0C0F	STX	FF 8002	
0C12	LDAA	B6 0CB1	Set peak current. Load accum. A with value of peak current and store in 8002.
0C15	STAA	B7 8002	
0C18	LDAA	B6 0CB2	Set steady current.
0C1B	STAA	B7 4002	
0C1E	JSR	BD 0CC1	Jump to Initialization sub.
0C21	JSR	BD 0C9D	Jump to Wait for Chopper to Close sub.
0C24	JSR	BD 0CA7	Jump to Wait for Chopper to Open sub.
0C27	LDAA	86 40	Connect capacitor of S&H and turn lamp to peak current.
0C29	STAA	B7 4000	
0C2C	LDX	FE 0CBB	
0C2F	DEX	09	Sample time loop for peak data acquisition.
0C30	BNE	26 FD	
0C32	LDAA	86 04	Turn lamp off and disconnect capacitor.
0C34	STAA	B7 4000	
0C37	STAA	B7 0C9C	Reference location.
0C3A	JSR	BD 0CE9	Jump to Data Acquisition sub.
0C3D	LDAA	86 24	Discharge capacitor.
0C3F	STAA	B7 4000	
0C42	LDX	FE 0CB7	Load index reg. with location where to store peak data value.
0C45	JSR	BD 0E27	Jump to Store Data sub.
0C48	STX	FF 0CB7	Save location where to store next value.
0C4B	LDX	FE 0CBD	
0C4E	DEX	09	Discharge time loop.
0C4F	BNE	26 FD	
0C51	JSR	BD 0CC1	Initialization sub.
0C54	JSR	BD 0CA7	Wait for Chopper to Open sub.
0C57	JSR	BD 0C9D	Wait for Chopper to Close sub.
0C5A	INC	01	
0C5B	INC	01	
0C5C	LDAA	86 44	Connect capacitor and keep lamp

0C5E	STAA	B7 4000	at steady current.
0C61	LDX	FE 0CBF	
0C64	DEX	09	Sample time loop for steady data
0C65	BNE	26 FD	acquisition.
0C67	LDAA	86 04	
0C69	STAA	B7 4000	Disconnect capacitor and keep
0C6C	STAA	B7 0C9C	lamp at steady current.
0C6F	JSR	BD 0CE9	Data Acquisition sub.
0C72	LDAA	86 24	
0C74	STAA	B7 4000	Discharge capacitor.
0C77	LDX	FE 0CB9	
0C7A	JSR	BD 0E27	Store steady data value.
0C7D	STX	FF 0CB9	
0C80	LDX	FE 0CBD	
0C83	DEX	09	Discharge time loop.
0C84	BNE	26 FD	
0C86	INC	01	
0C87	INC	01	
0C88	INC	01	
0C89	INC	01	
0C8A	INC	01	
0C8B	DEC	7A 0CB3	Decrement value of the number of
			sets of data to be taken.
0C8E	TST	7D 0CB3	Test to see if = 0
0C91	BEQ	27 03	
0C93	JMP	7E 0C1E	No - Jump to 0C1E to obtain another
			set.
0C96	JMP	7E 0D57	Yes - Jump to Addition sub.
0C99	INC	01	
0C9A	INC	01	
0C9B	INC	01	
0C9C	Ref. location		
			<u>Wait for Chopper to Close Sub.</u>
0C9D	LDAA	B6 4000	Load Accum. A with value in 4000.
OCA0	ANDA	84 08	AND with 08
OCA2	CMPA	81 08	Compare with 08
OCA4	BEQ	27 F7	Branch if equal back to obtain
			another value from 4000.
OCA6	RTS	39	Return
			<u>Wait for Chopper to Open Sub.</u>
OCA7	LDAA	B6 4000	Load Accum. A with value in 4000.
OCAA	ANDA	84 08	AND with 08
OCAC	CMPA	81 08	Compare with 08
OCAE	BNE	26 F7	Branch if not equal back to obtain
			another value from 4000.
OCB0	RTS	39	Return

OCB1 peak current value
 OCB2 steady current value
 OCB3 # data sets to be taken - 02, 04, 08, 10, 20, or 40
 OCB4 MSB initially 03
 OCB5 LSB1 initially 80
 OCB6 LSB2 initially 00
 OCB7 0F Location where store first peak data value.
 OCB8 70
 OCB9 0F Location where store first steady data value.
 OCBA FF
 OCBB 00 Sample time for peak data value acquisition.
 OCB8 80
 OCB9 00 Discharge time.
 OCBE 35
 OCBF 00 Sample time for steady data value acquisition.
 OCC0 80

Initialization Subroutine

OCC1	LDAA	86 00	
OCC3	STAA	B7 OCB6	Clear location OCB6.
OCC6	LDAA	86 03	
OCC8	STAA	B7 OCB4	OCB4 = 03
OCCB	LDAA	86 80	
OCCD	STAA	B7 OCB5	OCB5 = 80
OCD0	RTS	39	Return

OCD1, OCD4, OCD6, OCD7, OCDD, OCDE, OCE3-OCE6 are locations used in subroutines to hold data.

Data Acquisition Subroutine

OCE9	LDAA	86 00	
OCEB	STAA	B7 8000	Clear 8000
OCEE	LDX	CE 0020	Conversion time for D/A converter.
OCF1	DEX	09	
OCF2	BNE	26 FD	
OCF4	LDAA	B6 OCB4	Load Accum. A with MSB - initially 03.
OCF7	ADDA	BB OC9C	Add to the value in Accum. A the value in OC9C which will retain the S&H and lamp conditions.
OCFA	STAA	B7 4000	Store result into 4000.
OCFD	LDX	CE 0020	
OD00	DEX	09	D/A conversion time
OD01	BNE	26 FD	
OD03	LDAA	B6 4000	Load Accum. A with the value in 4000. AND with 10.
OD06	ANDA	84 10	
OD08	CMPA	81 10	Compare with 10.

OD0A	BNE	26 0B	Branch to OD17 if not equal - ref. voltage is smaller than unk.
OD0C	DEC	7A 0CB4	Decrement MSB
OD0F	TST	7D 0CB4	Test if = 0
OD12	BEQ	27 03	Branch to OD17 if equal to 0.
OD14	JMP	7E 0CF4	Otherwise test new MSB.
OD17	LDAA	B6 0CB4	
OD1A	ADDA	BB 0C9C	Store MSB + the value in 0C9C into
OD1D	STAA	B7 4000	4000.
OD20	LDX	CE 0020	
OD23	DEX	09	D/A conversion time
OD24	BNE	26 FD	
OD26	LDAA	B6 0CB5	Load Accum. A with the value of
OD29	STAA	B7 8000	LSB1 - initially 80 and store into
OD2C	LDX	CE 0020	8000.
OD2F	DEX	09	D/A conversion time.
OD30	BNE	26 FD	
OD32	LDAA	B6 4000	Test to see if the ref. is greater
OD35	ANDA	84 10	than or less than the unk.
OD37	CMPA	81 10	
OD39	BEQ	27 09	Branch to OD44 if ref. greater.
OD3B	LDAA	B6 0CB5	Load Accum. A with LSB1 and add to
OD3E	ADDA	BB 0CB6	it LSB2 (initially = 0).
OD41	STAA	B7 0CB6	Store sum into 0CB6.
OD44	CLC	0C	Clear carry.
OD45	ROR	76 0CB5	Divide LSB1 by 2.
OD48	CLC	0C	Clear carry.
OD49	LDAA	B6 0CB5	Load Accum. A with LSB1.
OD4C	TSTA	4D	Test LSB1 = 0 ?
OD4D	BEQ	27 06	Branch to OD55 if equal to 0.
OD4F	ADDA	BB 0CB6	Add LSB2 to LSB1.
OD52	JMP	7E 0D29	Jump to OD29 to test new LSB1.
OD55	RTS	39	Return
OD56	INC	01	
OD57	LDX	CE 0F70	Load index reg. with 0F70 -
OD5A	STX	FF 0CD4	location where LSB of first data
			value obtained is stored and store
			into 0CD4.
OD5D	LDX	FE 0CB7	Load index reg. with location of
			last MSB obtained.
OD60	JSR	BD 0D9C	Jump to Addition Sub.
OD63	STAA	B7 0CD7	0CD7 = MSB of sum.
OD66	STAB	F7 0CD6	0CD6 = LSB of sum.
OD69	JSR	BD 0DB4	Jump to Division Sub.
OD6C	LDAA	B6 0CD7	
OD6F	STAA	B7 0CE3	0CE3 = MSB of ave, peak value

0D72	LDAA	B6	QCD6	
0D75	STAA	B7	OCE4	OCE4 = LSB of ave. peak value.
0D78	LDX	CE	0FFF	Repeat for steady data value.
0D7B	STX	FF	OCD4	
0D7E	LDX	FE	OCB9	
0D81	JSR	BD	0D9C	Jump to Addition sub.
0D84	STAA	B7	OCD7	OCD7 = MSB of sum.
0D87	STAB	F7	OCD6	OCD6 = LSB of sum.
0D8A	JSR	BD	0DB4	Jump to Division sub.
0D8D	LDAA	B6	OCD7	
0D90	STAA	B7	OCE5	OCE5 = MSB of ave. steady value.
0D93	LDAA	B6	OCD6	
0D96	STAA	B7	OCE6	OCE6 = LSB of ave. steady value.
0D99	JMP	7E	ODFA	Jump to ODFA.

Addition Subroutine

0D9C	LDAA	A6	01	Accum. A = MSB
0D9E	INX		08	Increment index reg.
0D9F	LDAB	E6	01	Accum. B = LSB
0DA1	INX		08	
0DA2	ADDA	AB	01	Add next MSB to Accum. A.
0DA4	INX		08	
0DA5	CLC		0C	Clear carry.
0DA6	ADDB	EB	01	Add next LSB to Accum. B.
0DA8	INX		08	
0DA9	BCS	25	06	Branch to ODB1 if carry is set.
0DAB	CPX	BC	OCD4	Compare index reg. with value of location where LSB of first data value taken is stored.
0DAE	BNE	26	F2	Branch to ODA2 if not equal.
0DB0	RTS		39	Return
0DB1	INCA	4C		Increment Accum. A.
0DB2	BRA	20	F7	Branch to ODAB.

Division Subroutine

0DB4	LDAA	86	01	
0DB6	STAA	B7	OCDD	OCDD = 01
0DB9	LDAA	B6	OCDE	Load Accum. A with the number of data sets taken.
0DBC	LDAB	C6	02	Accum. B = 02
0DBE	CBA		11	Compare accumulators.
0DBF	BEQ	27	06	Branch to ODC7 if equal.
0DC1	ROLB		59	02 x 2
0DC2	INC	7C	OCDD	Increment the value in OCDD
0DC5	BRA	20	F7	Branch to ODBE
0DC7	LDAA	B6	OCD6	Accum. A = sum of LSB
0DCA	LDAB	F6	OCDD	Accum. B = # times to /2.
0DCD	CLC		0C	Clear carry.
0DCE	RORA		46	Divides LSB by 2.

ODCF	DECB	5A	Decrement Accum. B
ODD0	TSTB	5D	and test to see if = 0.
ODD1	BNE	26 FA	Branch to OCD1 if not = 0.
ODD3	STAA	B7 OCD6	OCD6 = remaining value in Accum.A.
ODD6	LDAA	86 00	
ODD8	STAA	B7 OCD1	OCD1 = 00
ODDB	LDDA	B6 OCD7	Accum. A = sum of MSB
ODDE	LDAB	F6 OCDD	Accum. B = # times to /2.
ODE1	CLC	0C	Clear carry.
ODE2	RORA	46	Rotate Accum. A to the right into
ODE3	ROR	76 OCD1	the carry and then rotate the
ODE6	DECB	5A	carry into OCD1. Decrement Accum.
ODE7	TSTB	5D	B and test to see if = 0.
ODE8	BNE	26 F7	Branch to ODE1 if not equal to 0.
ODEA	STAA	B7 OCD7	OCD7 = remaining value in Accum.
			A = ave. MSB.
ODED	LDAA	B6 OCD6	
ODF0	ADDA	BB OCD1	Accum. A = value in OCD1 + value
			in OCD6.
ODF3	STAA	B7 OCD6	OCD6 = Accum. A = ave. LSB.
ODF6	RTS	39	Return
ODF7	INC	01	
ODF8	INC	01	
ODF9	INC	01	
ODFA	LDAA	86 40	
ODFC	STAA	B7 OCB3	OCB3 = 40 = #sets of data to take
ODFF	STAA	B7 OCDE	OCDE = 40
OE02	LDAA	86 03	
OE04	STAA	B7 OCB4	OCB4 = 03
OE07	LDAA	86 80	
OE09	STAA	B7 OCB5	OCB5 = 80
OE0C	LDAA	86 00	
OE0E	STAA	B7 OCB6	OCB6 = 00
OE11	LDAA	86 70	
OE13	STAA	B7 OCB8	OCB8 = 70
OE16	LDAA	86 FF	
OE18	STAA	B7 OCBA	OCBA = FF
OE1B	LDAA	86 0F	
OE1D	STAA	B7 OCB7	OCB7 = 0F
OE20	STAA	B7 OCB9	OCB9 = 0F
OE23	RTS	39	Return
OE24	INC	01	
OE25	INC	01	
OE26	INC	01	

Store Data Subroutine

0E27	LDAA	B6 0CB6	Accum. A = LSB
0E2A	STAA	A7 00	Store in location specified by the index reg.
0E2C	DEX	09	Decrement index reg.
0E2D	LDAA	B6 0CB4	Accum. A = MSB
0E30	STAA	A7 00	Store
0E32	DEX	09	Decrement index reg.
0E33	RTS	39	Return

APPENDIX D

APPENDIX D

Tiny Basic Program

```
1  REM  PULSED HOLLOW CATHODE
2  REM  LAMP FOR ATOMIC ABSORPTION
3  REM  SPECTROSCOPY
4  REM
5  REM  JAMES B. SCHILLING
6  REM  JAN. 7, 1983
7  REM
8  PR "INPUT VALUE OF PEAK CURRENT"
9  INPUT A
10 B=USR(7192,3249,A)
11 PR "INPUT VALUE OF STEADY CURRENT"
12 INPUT A
13 B=USR(7192,3250,A)
14 L=0
15 M=0
16 PR "BLANK"
17 Q=5
18 GOSUB 72
19 Q=Q-1
20 IF Q >= 1 GOTO 18
21 Q=5
22 GOSUB 72
23 L=L+(G-F)
24 M=M+G
25 Q=Q-1
26 IF Q >= 1 GOTO 22
27 PR "ASPIRATE SAMPLE"," ",L,M
28 Q=5
29 GOSUB 72
30 Q=Q-1
31 H=Q
32 A=L
33 C=(G*5)-(F*5)
34 GOSUB 96
35 Z=10000-E
36 PR "%A="," ",Z
37 Z=M-(G*5)
38 PR "EMISSION="," ",Z
39 IF H > 0 GOTO 29
40 GOTO 14
```


Data Acquisition Subroutine

```
72      F=0
73      G=0
74      E=2
75      D=USR(3072)
76      A=USR(7188,3299)
77      B=USR(7188,3300)
78      C=USR(7188,3301)
79      D=USR(7188,3302)
80      A=A*256
81      C=C*256
82      B=B+A
83      D=D+C
84      REM
85      E=E-1
86      F=F+B
87      G=G+D
88      IF E > 0 GOTO 75
89      REM
90      REM
91      RETURN
```

Division Subroutine

```
96      E=0
97      T=A/10
98      P=1000
99      D=A-(T*10)
100     E=((C/T)*P)+E
101     B=(C/T)*T
102     C=((C-B)*10)-(D*(C/T))
103     P=P/10
104     IF P \ 0 GOTO 100
105     IF (C/T) > 5 GOTO 107
106     E=E+1
107     RETURN
```

APPENDIX E

APPENDIX E

MEMORY CHART

Tiny Basic

Location

- | | |
|-------------------------------------|--------|
| 1. Main Routine..... | 1-40 |
| 2. Data Acquisition Subroutine..... | 72-91 |
| 3. Division Subroutine..... | 96-107 |

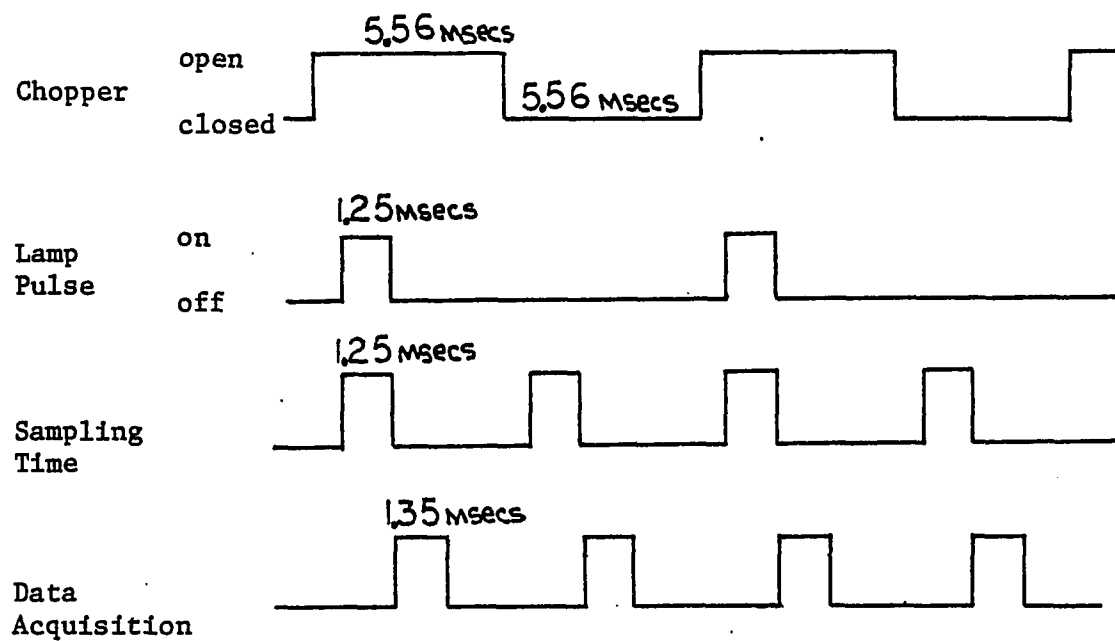
Machine Language

- | | |
|--------------------------------------------|-------------------------------------------------|
| 1. Main Routine..... | \$0C00-\$0C98
\$0D57-\$0D9B
\$0DFA-\$0E23 |
| 2. Initialization Subroutine..... | \$0CC1-\$0CD0 |
| 3. Wait for Chopper to Open Subroutine.... | \$0CA7-\$0CB0 |
| 4. Wait for Chopper to Close Subroutine... | \$0C9D-\$0CA6 |
| 5. Data Acquisition Subroutine..... | \$0CE9-\$0D55 |
| 6. Store Data Point Subroutine..... | \$0E27-\$0E33 |
| 7. Addition Subroutine..... | \$0D9C-\$0DB3 |
| 8. Division Subroutine..... | \$0DB4-\$0DF6 |

APPENDIX F

APPENDIX F

TIMING DIAGRAM



APPENDIX G

APPENDIX G

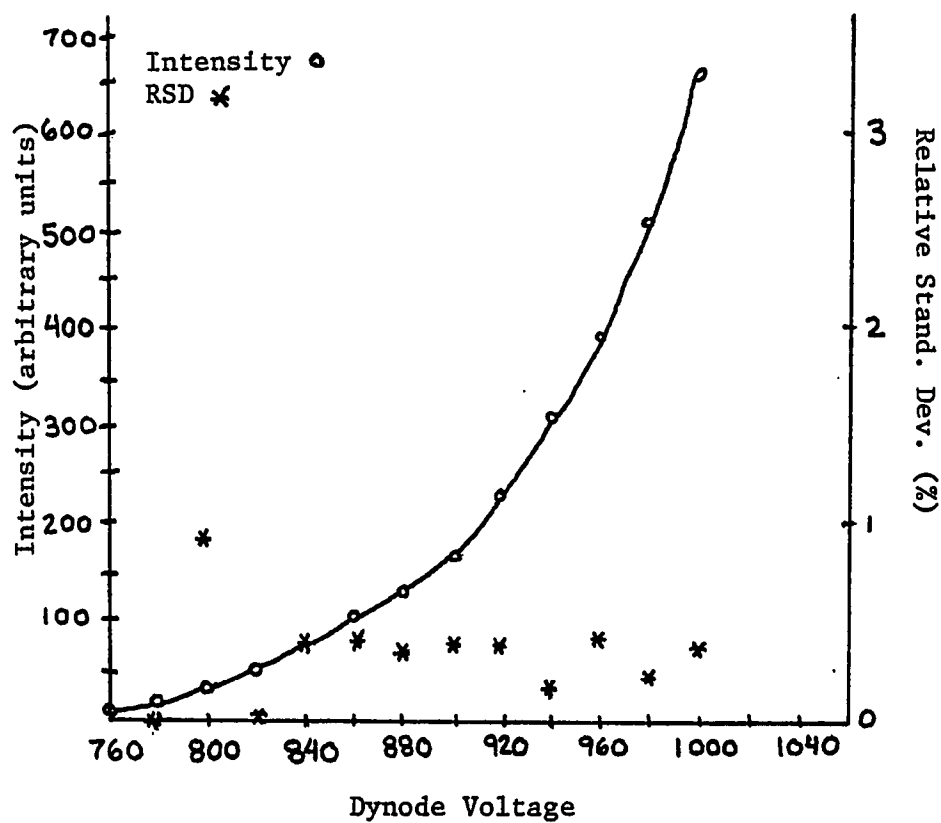


Figure G1. Plot of the dynode voltage of the PMT vs. the measured intensity of the Nickel hollow cathode lamp - Peak current 74 ma (30/250); wavelength 2320.0 Å; slit width 100 microns; 1P28 PMT.

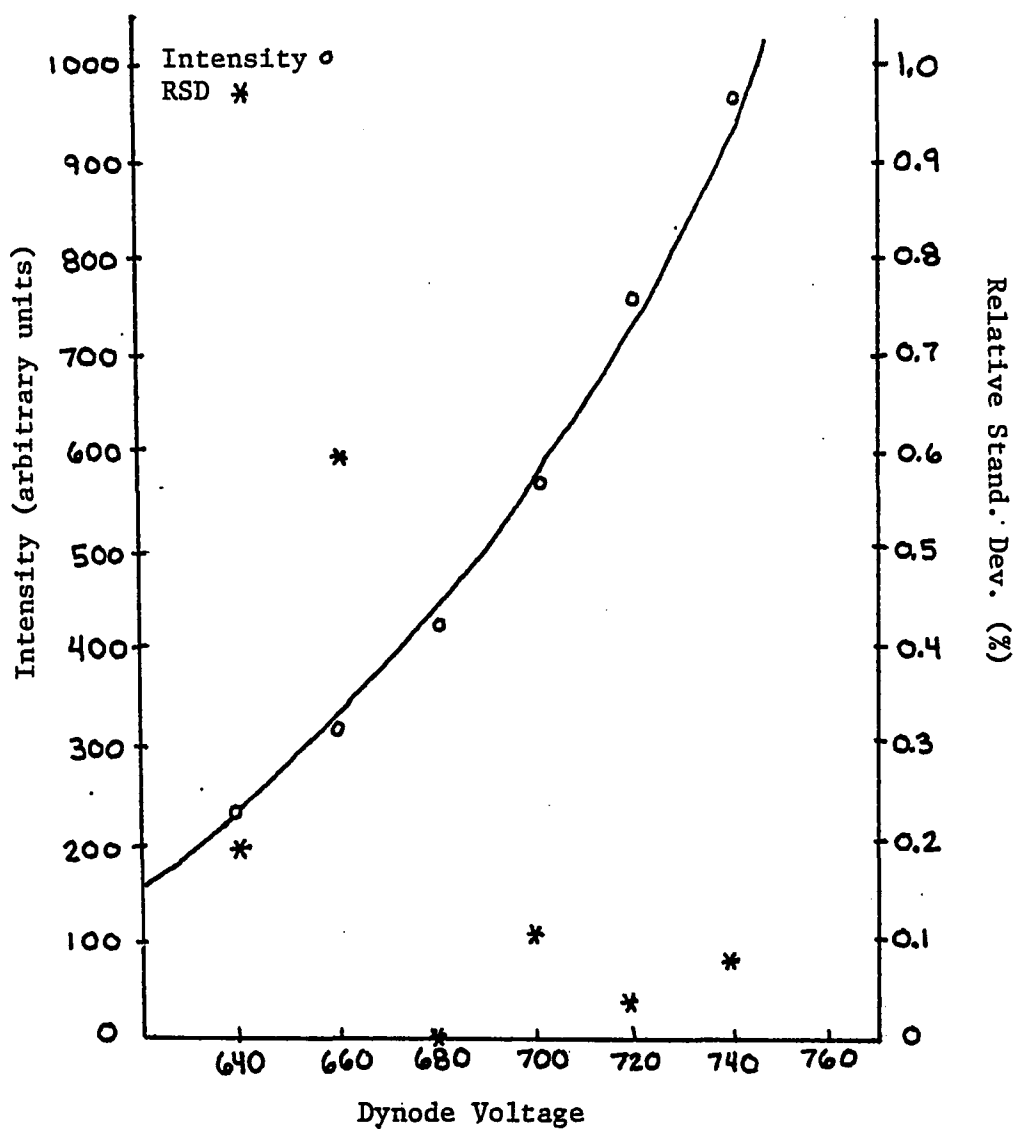


Figure G2. Plot of the dynode voltage of the PMT vs. the measured intensity of the Chromium hollow cathode lamp - Peak current 74 ma (30/250); wavelength 3578.7 Å; slit width 100 microns; 1P28 PMT.

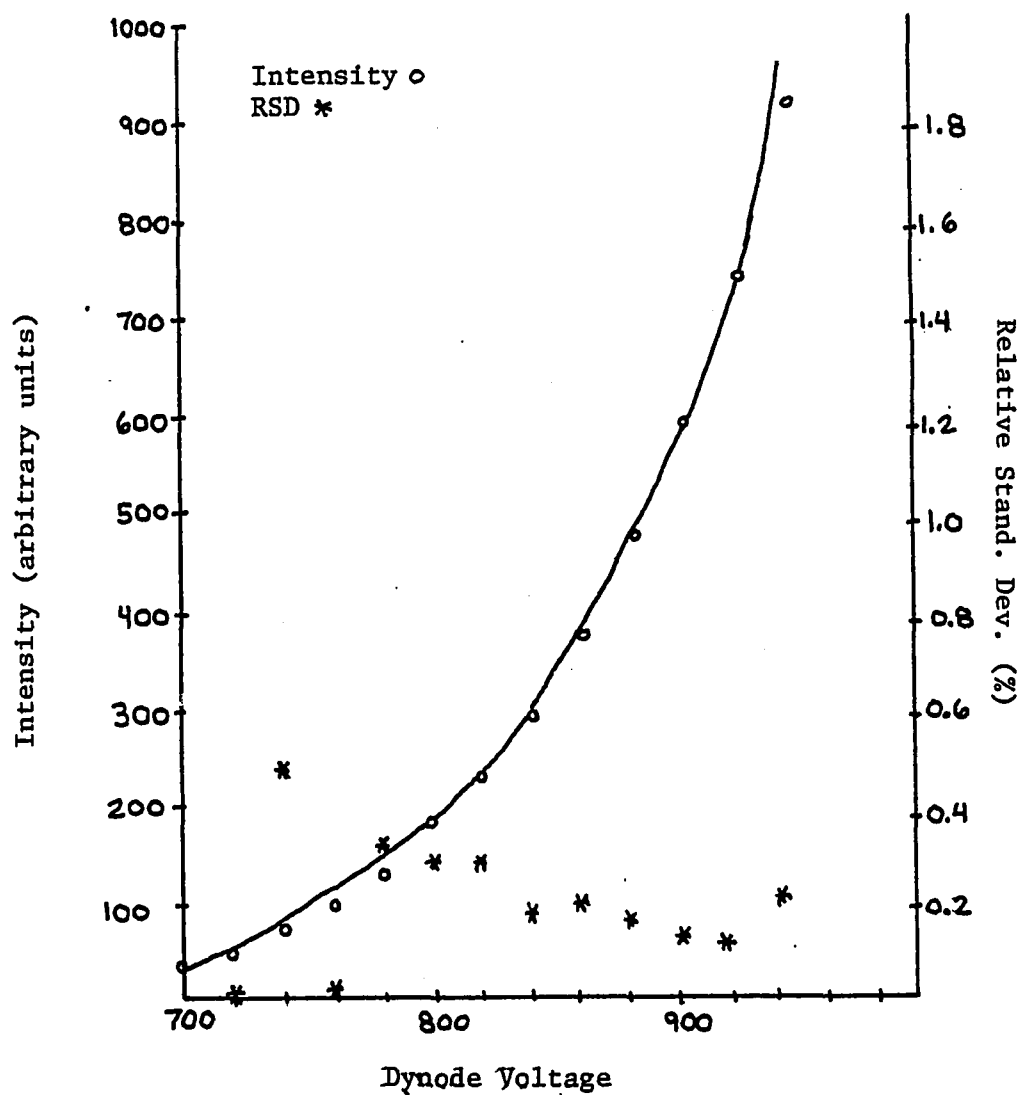


Figure G3. Plot of the dynode voltage of the PMT vs. the measured intensity of the Cobalt hollow cathode lamp - Peak current 74 ma (30/250); wavelength 2408.0 Å; slit width 100 microns; 1P28 PMT.

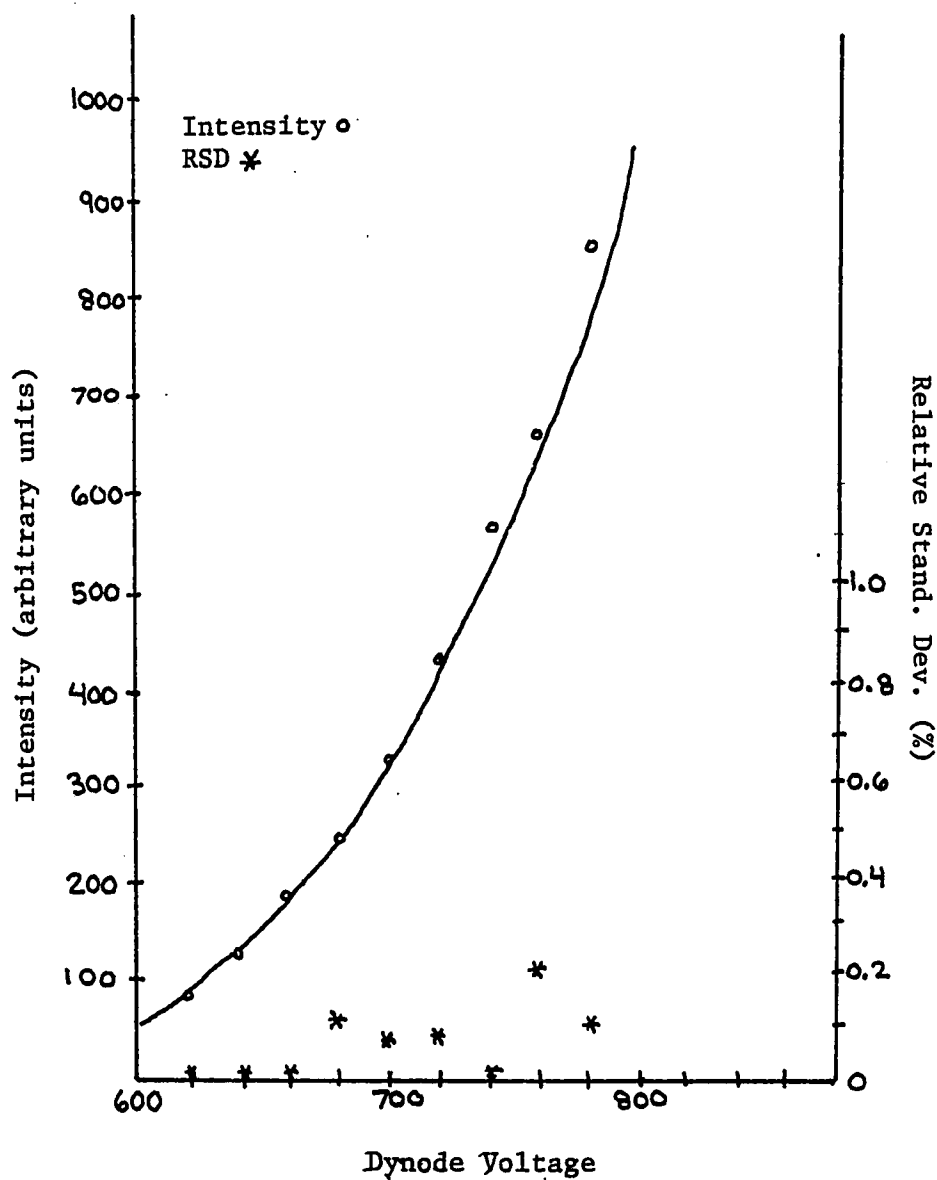


Figure G4. Plot of the dynode voltage of the PMT vs. the measured intensity of the Copper hollow cathode lamp - Peak current 74 ma (30/250); wavelength 3247.5 Å; slit width 100 microns; 1P28 PMT.

REFERENCES

1. Slavin, W. Atomic absorption spectroscopy the present and future. Anal. Chem., 1982, 54, 685A-694A.
2. Boumans, P.W.J.M. Atomic absorption spectroscopy past, present, and future. Spectrochim. Acta, 1980, 35B, No. 11/12.
3. Boumans, P.W.J.M. Atomic absorption spectroscopy past, present, and future. Spectrochim. Acta, 1981, 36B, No. 5.
4. Walsh, A. The application of atomic absorption spectra to chemical analysis. Spectrochim. Acta, 1955, 7, 108-117.
5. Walsh, A. U.S. Patent 2 847 899, 1958.
6. Rubeska, I., & Molden, B. Atomic absorption spectroscopy. Cleveland: The Chemical Rubber Co., 1969.
7. Christian, G.D., & Feldman, F.J. Atomic absorption spectroscopy applications in agriculture, biology, and medicine. New York: John Wiley and Sons Inc., 1970.
8. Dawson, J.B., & Ellis, D.J. Pulsed current operation of hollow cathode lamps to increase the intensity of resonance lines for atomic absorption spectroscopy. Spectrochim. Acta, 1967, 23A, 565-569.
9. Kitagawa, K., Suzuki, M., Aoi, N., & Tsuge, S. Analytical and spectral features of atomic magneto-optical spectroscopy (the atomic Faraday effect) of Sb, Bi, Ag, and Cu with a hollow cathode lamp operated in pulsed mode. Spectrochim. Acta, 1981, 36B, 21-34.
10. DeJong, G.J., & Piepmeier, E.H. Time- and wavelength- resolved emission line profiles for pulsed Cu and Ag hollow cathode lamps. Spectrochim. Acta, 1974, 29B, 159-177.
11. DeJong, G.J., & Piepmeier, E.H. Self-reversal in a copper pulsed hollow cathode lamp. Anal. Chem., 1974, 46, 318-319.
12. Osten, D.E., & Piepmeier, E.H. Atomic absorption measurements in a Q-switched laser plume using pulsed hollow cathode lamps. Appl. Spectrosc., 1973, 27, 165-170.
13. Araki, T., Uchida, T., & Minami, S. A dual wavelength atomic absorption spectrophotometer using a pulsed hollow cathode lamp. Appl. Spectrosc., 1977, 31, 150-155.

14. Omenetto, N. Pulsed sources for atomic fluorescence. Anal. Chem., 1976, 48, 75A-81A.
15. Cordos, E., & Malmstadt, H.V. Characteristics of hollow cathode lamps in an intermittent high current mode. Anal. Chem., 1973, 45, 27-32.
16. Cordos, E., & Malmstadt, H.V. Programmable power supply for operation of hollow cathode lamps in an intermittent current-regulated high intensity mode. Anal. Chem., 1972, 44, 2407-2410.
17. Johnson, E.R., Mann, C.K., & Vickers, T.J. Computer controlled system for study of pulsed hollow cathode lamps. Appl. Spectrosc., 1976, 30, 415-422.
18. Jenke, D.R., & Woodruff, R. Simultaneous emission/absorption analysis in constant temperature atomic spectroscopy. Appl. Spectrosc., 1982, 36, 686-689.
19. Dewalt, F.G., Amend, J.R., & Woodruff, R. A background correction system for atomic absorption spectrometry. Appl. Spectrosc., 1981, 35, 176-181.
20. Dewalt, F.G., Amend, J.R., & Woodruff, R. A stable pulsed hollow cathode lamp power supply. Appl. Spectrosc., 1979, 5, 460-462.
21. Dowd, G. A new programmable lamp current supply for atomic absorption spectrophotometry. Spectrosc. Let., 1973, 6, 223-229.